A Comprehensive Study on Coverage Path Planning Strategies for Autonomous Underwater Vehicles with Nadir Gap

Thesis submitted in partial fulfillment
of the requirements for the degree of

Master of Science
in
Computer Science and Engineering by Research

by

Nikhil Chandak
2019111040
`nikhil.chandak@research.iiit.ac.in`

International Institute of Information Technology
Hyderabad - 500 032, INDIA
June 2024

International Institute of Information Technology
Hyderabad, India

CERTIFICATE

It is certified that the work contained in this thesis, titled 'A Comprehensive Study on Coverage Path Planning Strategies for Autonomous Underwater Vehicles with Nadir Gap' by Nikhil Chandak, has been carried out under my supervision and is not submitted elsewhere for a degree.

Date	Adviser: Prof. Kamalakar Karlapalem
Date	Co-adviser: Prof. Charu Sharma

To my family and friends

Acknowledgments

I would like to take this opportunity to thank my advisors, family and some of the closest people in my life who have made my journey over the last few years enjoyable.

Firstly, I am fortunate that Prof. Kamalakar Karlapalem took me as a student under his guidance after my second year given the fact that he was not particularly taking dual-degree students at that time. I am grateful for the amount of time and effort he has dedicated towards me, not just in terms of advising my research but also in other aspects like my career and professional development. He has been extremely flexible and very supportive of my endeavors like exploring other research domains through internships. I have greatly enjoyed our extensive discussions and his prompt feedback has been quite useful. I believe working with him and others over the years has given me a glimpse of how to lead research directions and be self-motivated. I would also like to extend my gratitude to Prof. Charu Sharma for co-advising me. Her insights and low-level feedback has been very helpful.

During my time at IIIT, I made some of my closest friends today who have been a constant source of support and joy. Specifically, I would like to thank Keshav, Aman, Eshan, Adwait, Samay, Kunal, Naman, Shashwat, Rutvik and Siddhant. Each of you hold a special place in my heart and I am grateful to have friends like you.

Over the past few years, I am also grateful to have been in very close touch with my friends Sriesh, Yash, Ayush, Mudit, Teena, Neha, and Akash, whom I have known since school days.

Most importantly, I would like thank my mom and dad for always being there for me, my brother Yash for guiding in me every stage of life and my sister Raunak for personal and emotional support.

Abstract

Autonomous Underwater Vehicles (AUVs) play a vital role in exploring and mapping underwater environments. However, the presence of nadir gaps, or blind zones, in commercial AUVs can lead to unexplored areas during mission execution, limiting their effectiveness. We refer to the area under inspection not sensed by the AUV as **nadir gap**. We study the problem of underwater exploration of a rectangular region focusing on single and multiple AUVs with nadir gaps.

Complete exploration of a given area using such a AUV requires careful planning such that no area is left uncovered due to nadir gaps. Initially unexplored areas can be covered later using extra trips, but that may cause some areas to be covered multiple times leading to redundant *overlap* and ineffective resource usage. Hence, we devise strategies that not only cover the entire input area but also aim to minimize mission completion time and the total number of turns taken by the AUV(s). There has been extensive work on developing strategies which explore the entire area of interest but all of them are limited to exploration with a single AUV when nadir gap is a constraint. When multiple AUVs are available for deployment, the challenge is how to facilitate efficient collaboration among them while effectively compensating for the nadir gap and avoiding collision. A comprehensive study on efficient exploration of the entire region using *an arbitrary number of AUVs* each with nadir gaps is lacking in the literature. Our thesis aims to fill this gap by proposing scalable path planning strategies that offer complete coverage while minimizing either the mission completion time or the total number of turns performed.

Another challenge with the availability of multiple AUVs can be their unexpected failures. We take the first step towards addressing this challenge with two AUVs specifically and develop robust strategies which can handle the failure of a single AUV by effectively re-planning the path for the other (alive) AUV to obtain complete coverage. On the empirical front, we consider diverse input configurations based on real-world instances and provide extensive simulation results to validate the key properties of our strategies developed for single AUV, two AUV and multiple AUV scenarios. Further, we also show the maximal number of AUVs required that can be utilized fruitfully to achieve complete coverage for a given input (increasing the number of AUVs after this threshold doesn't decrease the overall completion time) and how to compute it efficiently. We end with a discussion of our most effective strategies from which a practitioner can select the best strategy based on the use case.

Contents

List of Figures

List of Tables

Chapter 1

Introduction

1.1 Motivation

Coverage path planning is a crucial task in various applications such as environmental monitoring, underwater exploration, and oceanographic surveys. The goal of coverage path planning is to generate a trajectory for a robot that can cover an area of interest efficiently and effectively. The importance of coverage path planning arises from the need to obtain complete and accurate information about the target area. In many applications, incomplete coverage can lead to incorrect interpretations and conclusions, which can have significant implications for decision-making.

Underwater applications such as environmental monitoring and oceanographic surveys require the collection of large amounts of data from various locations in the ocean. However, due to the vastness and complexity of the ocean, manually collecting data from different locations is not feasible. Autonomous Underwater Vehicles (AUVs)[1] offer an efficient and cost-effective solution to this problem by automating the data collection process. AUVs are unmanned underwater vehicles that can navigate autonomously through the water, collect data, and transmit it to the surface for analysis.

AUVs have several advantages over traditional manned vehicles. They can operate for extended periods without requiring human intervention, and they can access areas that are difficult or impossible for manned vehicles to reach. Additionally, AUVs are equipped with sophisticated sensor suites that can collect data with high accuracy and resolution, making them ideal for scientific research and environmental monitoring. However, AUVs face several challenges when it comes to coverage path planning. One of the most significant challenges is the presence of **nadir gaps**. In underwater applications, the presence of nadir-gaps, also known as *blind zones*, can significantly impact the effectiveness of the coverage path planning algorithm. Nadir gaps occur at the center and the area underneath that region of the vehicle cannot be directly observed due to the limitations of the sensor suite. Thus, nadir gaps present a unique challenge for coverage path planning algorithms. They occur due to the arrangement of the sensors based on the shape of the AUV .

[1]also known as Unmanned Underwater Vehicle (UUV).

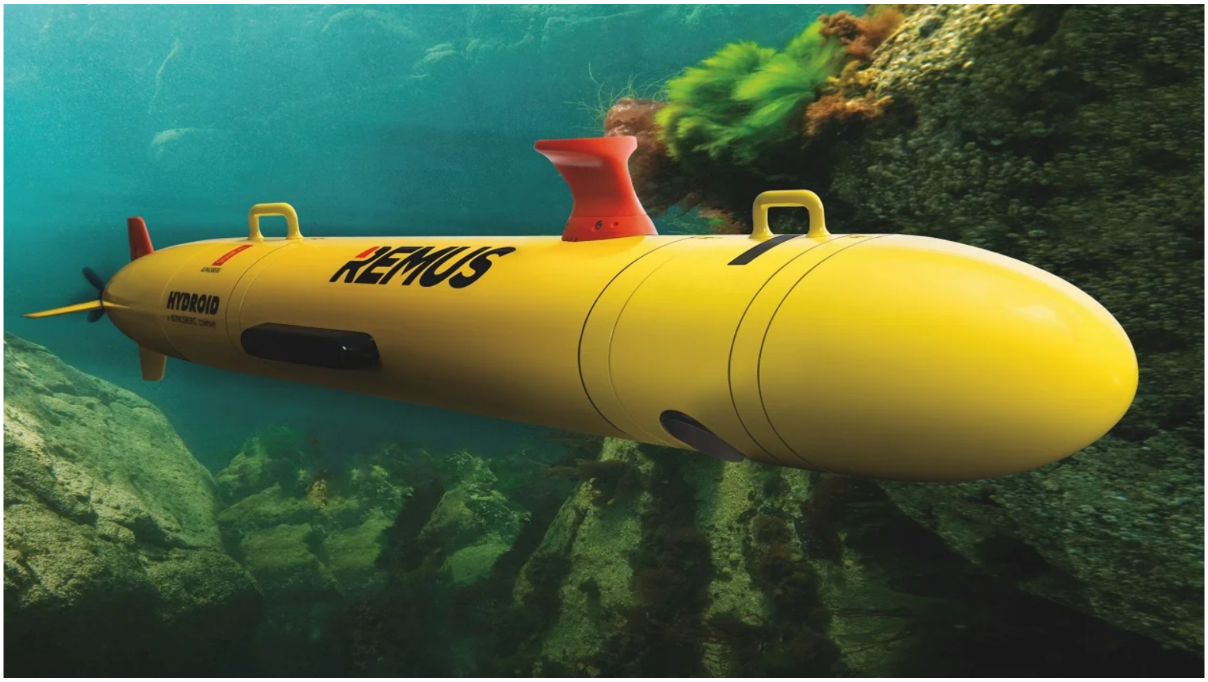

Figure 1.1: The vechicle shown in the image is REMUS 300, a two-man portable, small-class unmanned underwater vehicle (UUV). It can perform a range of missions including mine countermeasures (MCM), hydrographic survey and rapid environmental assessment (REA).REMUS (Remote Environmental Monitoring UnitS) is a series of autonomous underwater vehicles (AUVs). Image Credit: Hydroid.

1.2 Challenges

Nadir gaps can significantly impact the effectiveness of the coverage path planning algorithm. A coverage path planning algorithm may generate a trajectory that leaves large portions of the target area uncovered if the nadir gap is not taken into account. This can lead to incomplete data collection and inaccurate conclusions, which can have significant implications for decision-making.

To address the challenge of nadir gaps, approaches have been proposed for coverage path planning exclusively for single-AUV missions (Yordanova et al., 2019; Yordanova and Gips, 2020; Zhou et al., 2020; Morin et al., 2013). These methods (Yordanova et al., 2019; Yordanova and Gips, 2020) are mostly heuristic based and have only been developed for planning with only a single vehicle. Using a single AUV or robot to cover a large area can be time-consuming and inefficient. In contrast, the use of multiple AUVs can significantly improve the coverage speed and efficiency. In applications where nadir gaps are present, the use of multiple AUVs becomes even more critical. The AUVs can collaborate and cover each other's blind-spots, ensuring complete coverage of the target area.

However, coordinating multiple AUVs for coverage path planning is not without its challenges. The AUVs must be able to coordinate their movements effectively. They must also be able to work together to avoid collisions and ensure that the coverage path is optimal. Moreover, when nadir gaps are present, the AUVs must be able to detect and avoid them while still ensuring complete coverage of the target area. This requires sophisticated algorithms that can take into account the location and size of the blind-zones and generate trajectories that avoid them. Another challenge when using multiple AUVs for coverage path planning is the need to distribute the workload efficiently. Depending on the size and complexity of the target area, some AUVs may have to cover a larger area than others. Therefore, the workload must be distributed such that each robot is utilized optimally, and the coverage speed and efficiency are maximized.

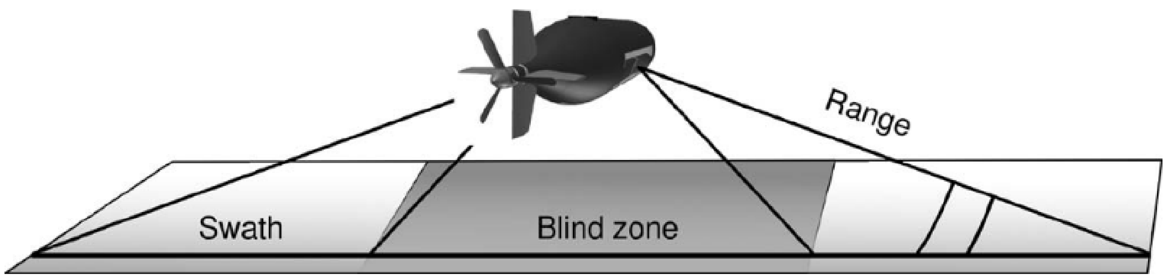

Figure 1.2: Typical imaging geometry of a Synthetic Aperture Sonar (SAS) used in AUVs. The port and starboard sonars have a very horizontal geometry, giving a blind zone underneath the vehicle. Typically in practice, the sensor swath is at least three times larger than the blind zone. The figure has been adapted from (Hansen et al., 2011, Figure 6)

One approach to addressing the challenge of nadir gaps is to use advanced sensor suites that can provide complete 360-degree coverage. These sensor suites typically consist of a combination of cameras, sonars, and other sensors that can provide complete coverage of the target area. However, such sensor suites can be expensive and require significant computational resources, making them less practical for many applications.

The impact of nadir gaps on coverage path planning is not limited to underwater applications. Nadir gaps are also a significant challenge in aerial and ground-based applications. In aerial applications such as surveillance and mapping, nadir gaps can occur due to the shape of the vehicle, the arrangement of the sensors, or the presence of obstacles such as buildings or trees. In ground-based applications such as agriculture and mining, nadir gaps can occur due to the shape of the vehicle, the terrain, or the presence of obstacles such as rocks or vegetation.

Thus, coverage path planning is a crucial task in various applications such as environmental monitoring, underwater exploration, and oceanographic surveys. The presence of nadir gaps presents a unique challenge for coverage path planning algorithms, which require the development of novel techniques that can address this challenge effectively. The development of effective coverage path planning algorithms that can account for nadir gaps and efficiently coordinate multiple AUVs is of great importance and has the potential to revolutionize the way we collect data and monitor our environment.

Figure 1.3: US Navy sailors lower a REMUS 600 into the water during a mine countermeasures exercise. Source: Wikipedia.

1.3 Key Contributions

Motivated by the aforementioned challenges, we devise *complete* coverage strategies for single and multiple AUVs. We briefly summarize our contributions below:

1. We first lay the foundations of the thesis by discussing several provably complete strategies for path planning with a single AUV. Among them, the strategy called `Complete Zigzag` is same as the survey pattern for maximum area coverage in Hagen and Hansen (2007). `Complete Zigzag` is often used in practice (Hagen and Hansen, 2007; Hagen, 2011; Yordanova and Gips, 2020). We take the first step in studying how close it would be to an optimal solution by theoretically analyzing the minimum overlap that would be incurred by any complete strategy using a single robot with blind zones and conjecture that `Complete Zigzag` is optimal in terms of least overlap.

2. We propose different techniques to extend `Complete Zigzag` to two AUVs depending on the specific objective like minimizing the number of turns taken or the maximum distance travelled by any AUV, while ensuring provably complete coverage.

3. We also provide fault-tolerant variant of our two-AUV strategies for failure-aware planning. Each such strategy is developed for optimizing specific metrics (like total number of turns or completion time) while offering full coverage.

4. We develop algorithmic techniques to scale the methods introduced for two AUVs to an arbitrary number of AUVs based on the specific metric to be optimized for.

5. We provide simulation results for various input configurations, based on actual field-experiments, for *one, two,* and *multiple* AUVs, validating the key properties of our strategies empirically.

1.4 Thesis Organization

The thesis is divided into 9 chapters. Chapter 2 introduces the background and relevance of the problem in the literature and briefly mentions the related work on coverage path planning using AUVs with nadir gaps. Chapter 3 introduces the formal problem formulation and how the nadir gap is modelled and also discusses our setup for evaluation using simulation. Chapter 4 presents various strategies, provably complete and non-complete, for coverage path planning with a single AUV. For complete strategies, we provide conditions in which they will always achieve full coverage. In Chapter 5, we extend the problem to two AUVs. We discuss how to effectively plan paths for the AUVs based on the optimization metric like maximum distance travelled and total number of turns performed. In Chapter 6, we develop robust strategies for two AUVs which can handle the failure of one AUV and effectively re-plan the path of other (alive) AUV to obtain complete coverage. In Chapter 7, we study the generalized version of our problem of coverage path planning with nadir gaps for an *arbitrary number of AUVs*. We provide technical details on how to effectively scale previous strategies introduced for two AUVs to multiple AUVs. For each of the chapters from 4 to 7, we also provide extensive simulation results for the strategies developed under various input configurations. We finally conclude the thesis with a discussion in Chapter 8 and provide research directions for future work in Chapter 9.

Chapter 2

Literature Review

2.1 Preliminaries

Recent rise in the interest in autonomous vehicles (AVs) with their utility in a broad range of applications has sparked an increase of research in the area of robot planning and multi-robot systems. AVs or robots received huge attention from a wide gamut of domains such as robotics, healthcare, e-commerce, transportation, agriculture, etc., with noteworthy problems including surveillance Casbeer et al. (2006) and monitoring systems Merino et al. (2012); DeBusk (2010), search and rescue operations Waharte and Trigoni (2010), industrial inspection Nikolic et al. (2013), cleaning robots Yasutomi et al. (1988), to name a few.

Coverage path planning (CPP) Cao et al. (1988) is one such fundamental problem in robotics that impacts several applications in the field. CPP algorithms determine the path taken by a robot in order to obtain the full coverage of an area. To cover the entire area, multiple robots can also collaborate for efficient coverage while minimizing a chosen cost function. The two main components of the CPP algorithm are viewpoints and path coverage. Viewpoint deals with the position and orientation of the robot while the path coverage depends on the optimal approach for coverage completeness. There are constraints based on the task and its requirements associated with the CPP problem with challenges to come up with the best approach. For example, one of the constraints considered in CPP problem is presence of obstacles in the area of interest (AOI) which has been studied extensively in the literature. The obstacles can either be static or moving and should be avoided for exploration. Furthermore, in the case of multiple robots, requirement can be to maintain a minimum safety distance between AVs to avoid any collisions.

To address these constraints, various approaches have been proposed to achieve full coverage with a collision-free path. The most commonly used approaches can be classified as grid-based Xu et al. (2014); Avellar et al. (2015); Kong et al. (2006), geometric-based Adaldo et al. (2017); Hassan and Liu (2017); Balampanis et al. (2017), reward-based Palacios-Gasós et al. (2017); Kapanoglu et al. (2012). Grid-based approaches include cell decomposition methods that divide the area of interest into cells in different ways and find the optimal solution on the basis of the initial position, number, and capabilities of robots. Methods of this category also utilize the idea of spanning tree and ant colony optimization methods. Geometric-based approaches make use of graphs to generate the path. Such methods consider Voronoi diagrams and apply graph search algorithm, shortest path algorithm, etc. Reward-based approaches are mostly based on neural network architectures. The rest of the approaches belong to the different categories depending on the availability of information beforehand Manjanna et al. (2018), shape and size of obstacles Lumelsky et al. (1990), using non-complex methods Choset (2001).

2.2 Related Work

While Coverage Path Planning (CPP) (Cao et al., 1988) is a fundamental problem in robotics, we focus our attention to CPP approaches specifically for underwater surveillance missions using AUVs with nadir gap. There has been extensive work on developing strategies which explore the entire area of interest but all of them are limited to exploration with a single AUV (Yordanova et al., 2019; Yordanova and Gips, 2020; Zhou et al., 2020; Morin et al., 2013). When multiple AUVs are available for deployment, the challenge is how to facilitate efficient collaboration among them while effectively compensating for the nadir gap. A comprehensive study on efficient exploration of the entire space using *an arbitrary number of AUVs* each with nadir gaps is lacking in the literature. Our work aims to fill this gap by proposing scalable path planning strategies that account for nadir gap and offer complete coverage while minimizing either the mission completion time or the total number of turns performed. Our techniques provide insights for efficient utilization of multiple AUVs, a critical aspect for large-scale exploration missions.

As we take the first steps towards addressing the challenges arising from the deployment of multiple AUVs in the context of CPP, we focus on the fundamental setting with static rectangular seabed and reliable sensory observations. While we consider the sonar detector to be perfect, several works in the literature have considered an imperfect detector defining a probability distribution over the sensor range for mine detection (Abreu et al., 2017; Morin et al., 2013; Zhou et al., 2020; Cai et al., 2022). In (Yordanova et al., 2019), a heuristic method is developed to maximize coverage at the tail of sensor range and dynamically adjust track spacing based on real-time sensor updates. Another study extended this concept by also incorporating the seabed type to model the mine detection probability(Williams, 2010). These techniques are complimentary to our work.

Researchers have also explored the impact of sand ripples on track orientation to optimize sensor visibility and minimize turns, thereby improving data quality for mine detection (Yordanova et al., 2019). Synthetic Aperture Sonar (SAS) has garnered attention, with investigations into performance metrics, area coverage rates, and survey patterns (Hagen and Hansen, 2007). Notably, survey pattern for maximum area coverage in (Hagen and Hansen, 2007) is same as our `Complete Zigzag` strategy for single AUV which we extend to multiple AUVs. Specific challenges associated with SAS for seafloor imaging have been discussed in (Hansen et al., 2011), emphasizing the need for robustness. Investigations have also been made on a number of possible 'gap-filling' sensors and their limitations with the broad conclusion that addition of such technology significantly increases the cost and complexity of the system making them unsuitable for most practical applications (Hagen, 2011).

Chapter 3

Problem Description and Evaluation

3.1 Background

Our study makes similar considerations as past works (Fang and Anstee, 2010; Yordanova et al., 2019; Yordanova and Gips, 2020) in respect to the AUV's capabilities, its sensor and the environment. We consider such family of vehicles which are designed to travel long distances particularly in a straight line and under water at constant speed and altitude. They are *not designed to follow curved paths and cannot detect or avoid obstacles*. We consider the AUV's survey sensor to be a high-resolution interferometric sidescan sonar such as Synthetic Aperture Sonar (SAS) (Hansen et al., 2011). Such sensors have a nadir range (dB in Fig. 3.1) and a maximum operational sonar range with a (user-defined) threshold determining the *admissible limit* (dS in Fig. 3.1) of the (imagery) data collected. Setting this threshold is outside the scope of our work but can be done either manually or automatically (Yordanova and Gips, 2020) to conservatively consider only the length with useful sensing capability. While prior works have considered both perfect (Hagen and Hansen, 2007; Fang and Anstee, 2010) and imperfect sensors (Yordanova and Gips, 2020; Morin et al., 2013; Williams, 2010; Cai et al., 2022), we consider perfect sensor which results in a binary performance, *i.e.*, the probability of detection is 1 for areas encompassed by the sonar swath and 0 otherwise. Similar to (Yordanova and Gips, 2020), we consider environments that are predetermined and remain static throughout the mission. We consider the seabed to be flat and horizontal; consequently, we confine our experiments to a rectangular shape[1]. Further, in such survey missions, the aspect of avoiding obstacles can generally be disregarded, as is the case for MCM (Yordanova and Gips, 2020; Fang and Anstee, 2010). The (problem) input is a set of coordinates delineating the survey area while the output is a sequence of waypoints outlining the path (survey leg) for each AUV. Some of these waypoints mark the location where turns take place and all turning maneuvers are confined to a predetermined radius around these waypoints[2].

[1]We note that our methods while developed for rectangular `AoI` can be extended to general polygonal shapes using decomposition methods like (Fang and Anstee, 2010) or by adapting track orientation like (Yordanova et al., 2019), which we leave for future work.

[2]We consider that the overhead distance in performing a turn has small variance and is (upper) bounded by a fixed maximal distance.

3.2 Objectives

Our primary objective is to ***(a)** achieve **complete** coverage of the area of interest (*`AoI`*)*. The analysis of sidescan sonar images is based on the consideration that the scan lines are evenly spaced and parallel, indicating that they are collected while each vehicle moves in a straight line at a constant speed; hence, the vehicle which travels the maximum distance dictates the mission completion time. One crucial metric in this regard is minimizing the time required to complete the mission. This becomes particularly significant when multiple vehicles are available, as more vehicles should lead to reduced completion time. To quantify this, we measure the maximum distance traveled by any vehicle since all vehicles have the same speed. Thus, the next objective we desire is ***(b)** minimizing the maximum distance travelled by any of the AUVs.* Further, the vehicle we consider is *not designed to follow curved trajectories and **any imagery obtained during turns is deemed unreliable** and is not taken into account for coverage*. Thus, another subsequent objective is to ***(c)** minimize the total number of turns made by the AUVs*. These metrics – (a), (b), (c) – are same as the ones studied extensively in prior works (Yordanova et al., 2019; Yordanova and Gips, 2020) to compare mission efficiency for the application of MCM. We note that **(a)** *achieving complete coverage* is the primary objective while metrics **(b), (c)** represent secondary objectives. Further, each (secondary) objective represents a distinct aspect of the mission, and *optimizing for one may compromise the other* (Yordanova et al., 2019). Thus, there may not be a single strategy optimal across all the objectives. We develop strategies tailored for each objective, empirically analyze their performance and report the best strategy depending upon the practitioner's desiderata.

3.3 Formulation

We are interested in the coverage of planar underwater environments using AUVs. Formally, we define our problem of *offline* exploration using AUVs with nadir gaps in two-dimensional environment (without obstacles) using the following tuple $\langle \mathcal{R}, N, \mathcal{S}, v, dS, dB \rangle$:

- $\mathcal{R}$ denotes the rectangular `AoI` of size $L \times B$ in the global frame whole of which needs to be covered once. For ease of planning, we transform $\mathcal{R}$ such that its bottom-left corner is at $(0, 0)$ coordinate on a 2D plane. In practice, both the length L and breadth B of the mission area are typically between $1 - 10$ kilometers long (Yordanova et al., 2019; Yordanova and Gips, 2020).
- N is the number of AUVs available for planning.
- $\mathcal{S}$ is the list of AUV deployment locations where $\mathcal{S}_i$ is a tuple (x_i, y_i) denoting the starting and returning coordinate for the i^{th} AUV. The size of $\mathcal{S}$ is N.
- v is the (constant) speed at which each AUV travels.
- dS is the length of sensor footprint covered by the vehicle perpendicular to its direction of motion. We model it as a scalar quantity on both sides of the motion (Fig. 3.1b).

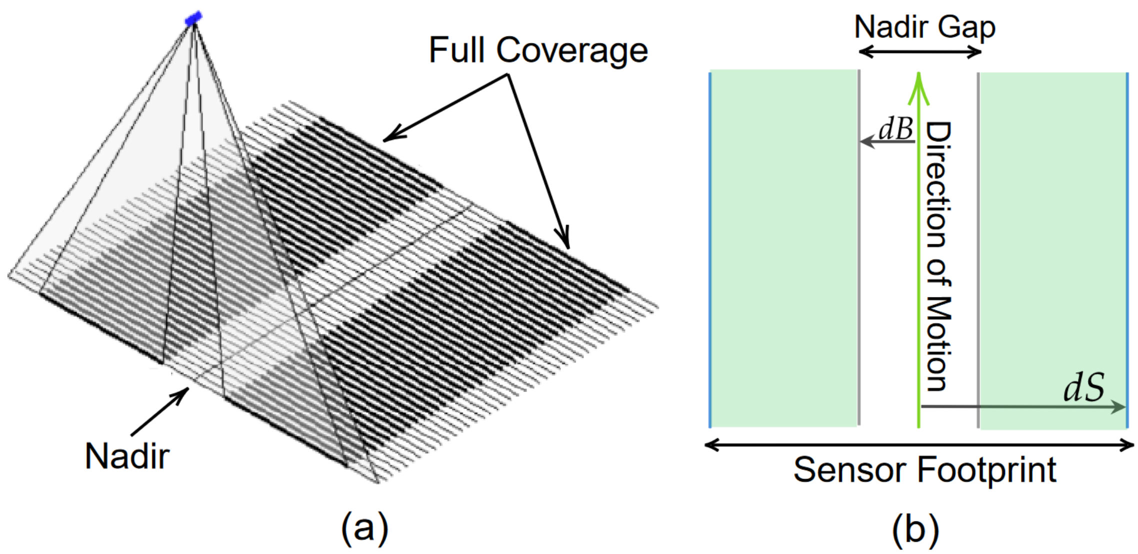

Figure 3.1: (a) This subfigure is taken from (Fang and Anstee, 2010) depicting an elevated perspective of the seafloor coverage through sidescan sonar, highlighting a distortion in coverage near the center (nadir). (b) Illustration of the nadir gap as a subsection of sensor footprint in our modelling of an AUV's survey sensor. Typically, the ratio between dS and dB is $3:1$ (Yordanova and Gips, 2020) with dS being a few hundred meters long. As the AUV travels, *only* the green region is covered.

- dB denotes the distance of blind zone left by the vehicle perpendicular to its direction of motion, modelled similarly as dS (Fig. 3.1b).

We note that value of dS (sensor range) and dB (nadir range) is specific to the AUV considered for deployment. For instance, consider the Mine-hunting UUV for Shallow-water Covert Littoral Expeditions (MUSCLE) — a Bluefin-21 autonomous underwater vehicle, equipped with a side-looking synthetic aperture sonar (SAS) (Baralli et al., 2013). Yordanova and Gips (2020) used MUSCLE in their field experiments for mine countermeasures and report that its SAS has nadir gap width of $40m$ per side (dB) with the sensor range being $130m$ per side (dS).

3.4 Evaluation Setup

To evaluate the performance of the coverage strategies we propose later, we perform simulations on diverse input parameters. All the experimental analysis was conducted in Python 3.7 on a laptop running Ubuntu 20.04, with 8 GB of RAM and an Intel i7-8700k processor. Our setup is based on actual field experiments from prior works (Yordanova and Gips, 2020; Yordanova et al., 2019) where the authors use the Mine-hunting UUV for Shallow-water Covert Littoral Expeditions (MUSCLE) — a Bluefin-21 AUV (Baralli et al., 2013) – equipped with a side-looking synthetic aperture sonar (Baralli et al., 2013) with nadir gap of 40 meters per side (dB) and (estimated) sensor range of 130 meters (dS) operated on a mission area of size 400×1212 meter^2. We use similar measurements in our experiments but scale them

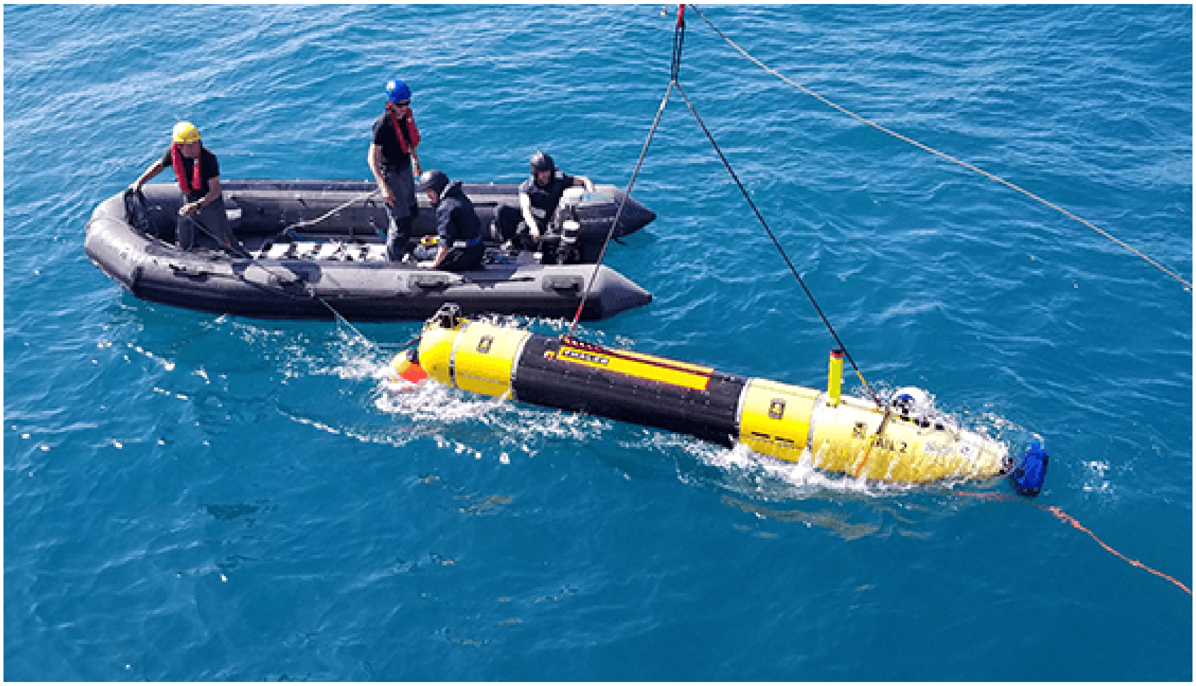

Figure 3.2: The MUSCLE (Minehunting UUV for Shallow waters Covert Littoral Expeditions) is a state-of-the-art mine hunting autonomous underwater vehicle, which uses multi-resolution, multi-aspect Synthetic Aperture Sonar to create detailed images of the sea floor. In the picture, NATO STO Centre for Maritime Research and Experimentation (CMRE) staff work with the MUSCLE vehicle during MINEX 2018 and Dynamic Mariner 2019 sea trials. Source: OCEAN2020 (Open Cooperation for European mAritime awareNess)

down for convenience in simulating. Particularly, we consider two kinds of environment with roughly similar total area:

1. A rectangle of size 20×15 units.

2. A square of of size 17×17 units.

In both the instances, a range of $dB \in \{0.1, 0.2, 0.3\}$ and $dS \in \{1, 2, 3\}$ values were considered.

Following our objectives devised in the past section, for each strategy, we measure 1) the maximum distance travelled by any of the AUVs and 2) the total turns made by the vehicles. Our experimental findings compliment the theoretical coverage guarantees of the strategies by demonstrating their performance on other important metrics. We also report the *overlap* incurred to quantify the (redundant) area covered more than once in the simulations for single AUV strategies. The results for different number of AUVs are reported in their respective chapters.

Chapter 4

Exploration with a single AUV

4.1 Motivation

In this chapter, we lay the foundation for coverage path planning with nadir gaps. In particular, we focus on path planning with a **single** AUV. Single AUV operations allow for a focused examination of the vehicle's capabilities, sensor coverage, and the effectiveness of different path planning strategies in mitigating the impact of nadir gaps. Even with a single AUV, addressing nadir gaps is a challenge. The physical and operational constraints of the AUV limit its maneuverability and the angles at which it can capture data, leading to unavoidable blind zones. We need to ensure that the AUV covers the entire area of interest efficiently, without unnecessary overlaps or revisits to already surveyed regions. By comprehensively studying the strategies for planning with a single AUV, we lay the groundwork for scalable solutions that can be adapted to fleets of AUVs, enhancing coverage efficiency in larger scale operations. We first restate the problem description, review prominent strategies from past work and also discuss strategies which achieve *complete coverage*.

4.2 Problem Formulation

In this chapter, we are are interested in the coverage of planar underwater environments using a single AUV. As stated earlier (in Chapter 3.3), we define our problem of *offline* exploration in two-dimensional environment using the following tuple $\langle \mathcal{R}, N, \mathcal{S}, v, dS, dB \rangle$:

- $\mathcal{R}$ denotes the rectangular `AoI` of size $L \times B$ in the global frame whole of which needs to be covered once.
- N is the number of AUVs available for planning. Here, $N = 1$.
- $\mathcal{S}$ is the list containing the AUV deployment location which is a tuple (x, y) denoting the starting and returning coordinate for the AUV.
- v is the (constant) speed at which each AUV travels.

- dS is the length of sensor footprint covered by the vehicle perpendicular to its direction of motion. We model it as a scalar quantity on both sides of the motion (Fig. 3.1b).

- dB denotes the distance of blind zone left by the vehicle perpendicular to its direction of motion, modelled similarly as dS (Fig. 3.1b).

Our objective is to achieve complete coverage of $\mathcal{R}$ while minimizing the mission completion time. For a single AUV, minimizing completion time is equivalent to minimizing the distance travelled by the AUV to achieve full coverage.

4.3 Strategies

We now discuss several coverage strategies. We first present simple geometric sweep patterns based on existing literature (Lumelsky et al., 1990; Choset and Pignon, 1998) and show that they do not achieve full coverage of the entire `AoI`. We next tweak these simple strategies to make them complete and later present strategies which cover the whole `AoI` under certain characteristics of the AUV, satisfied in our problem formulation.

4.3.1 Zigzag (Incomplete)

The most popular technique employed in prior works (Lumelsky et al., 1990; Choset and Pignon, 1998; Coombes et al., 2017) is the zigzag pattern. It involves back-and-forth motions resembling 'mowing the lawn' in either a horizontal or vertical direction based on the orientation of the `AoI` (Fig. 4.1). This strategy however is inconsiderate of the nadir gap. While it requires the least number of turns as it covers the maximum stretch possible in one trip, it leaves rectangular strips unexplored due to the AUV's nadir gap, resulting in *incomplete coverage*. We use this strategy as lower bound in our experiments for single AUV as it essentially treats dB to be 0 and would be optimal if there was no nadir gap.

4.3.2 Diagonal Zigzag (Incomplete)

Another way to perform the zigzag motion is to start near one of the corners of the rectangle and do back and forth exploration diagonally. When zigzag motion is performed diagonally, the stretch covered in one trip is not of the same length always. It keeps increasing initially until it reaches a maximal point after which it decreases. This strategy also leaves unexplored several disconnected regions from the `AoI` and requires more turns as the stretch covered in one trip is not maximal consistently.

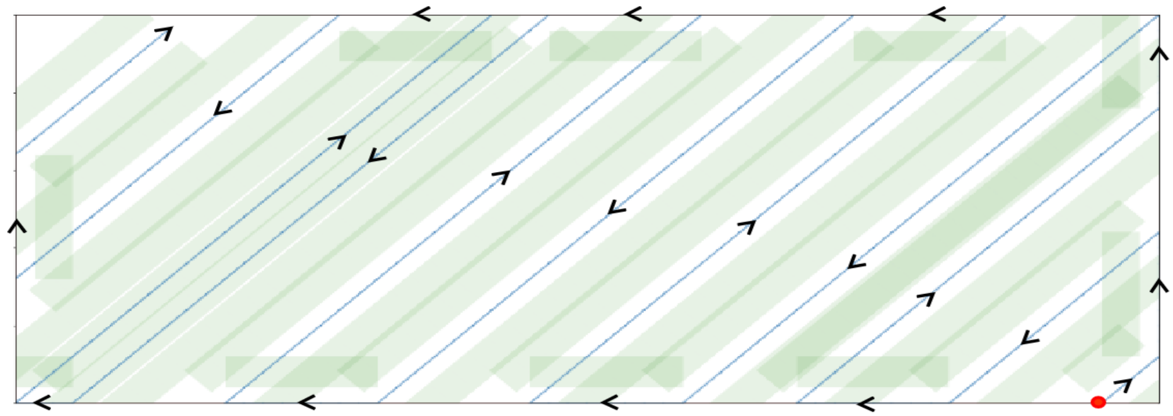

(a) Diagonal Zigzag

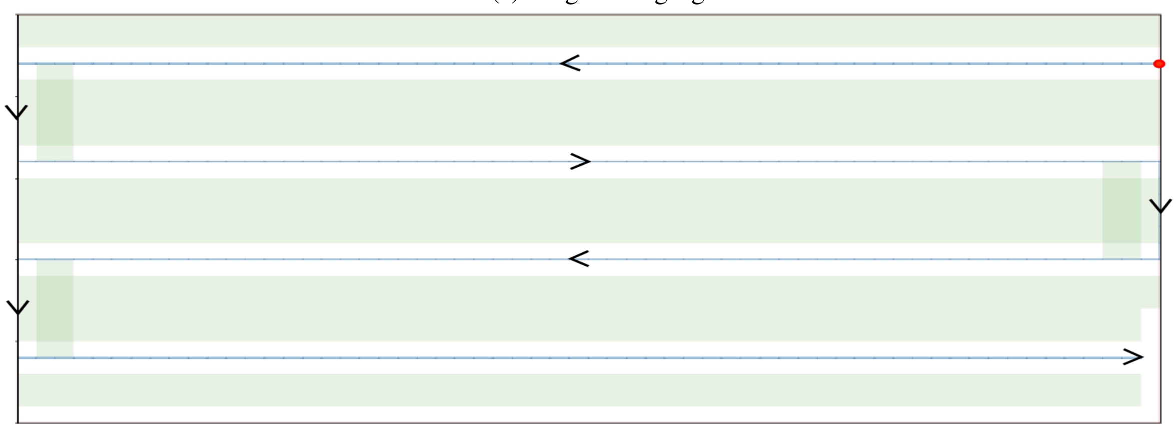

(b) Horizontal Zigzag

Figure 4.1: Coverage footprint (shown in light green strips) of a single AUV with blind zone whose trajectory is shown in light blue. Red dot denotes the starting point while black arrows denote the direction of motion. The white strips represent the area not explored by the AUV. *We note that the actual turns of an AUV are not sharp but are performed in the shape of an arc.*

4.3.3 No Gaps (Complete)

We now present our first complete strategy. Notice that at least a part of the sensor footprint (on either side) is continuous and complete so we can try using only one side of the footprint for coverage which is free of blind-zone. We can perform the above discussed zigzag motion by starting at $(-dB, 0)$ facilitating the right sensor footprint to cover a continuous strip (Fig. 4.2a) though the left footprint becomes futile as it covers redundant area (either outside $\mathcal{R}$ or already explored). Turns are made at the point where the other side of the footprint starts covering the area exactly where it was left off (Fig. 4.2b). We note that this strategy trivially achieves full coverage as it considers only one side of sensor footprint which offers complete coverage.

Corollary. `No Gaps` *strategy achieves full coverage of $\mathcal{R}$ irrespective of the size of the nadir gap (value of dB).*

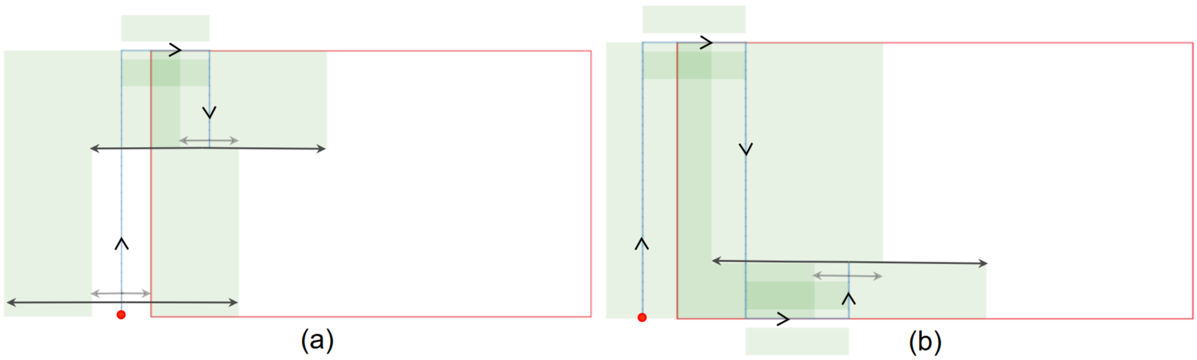

Figure 4.2: Illustration of an in-progress No Gaps strategy performed by a single AUV with blind zone.

4.3.4 Return (Complete)

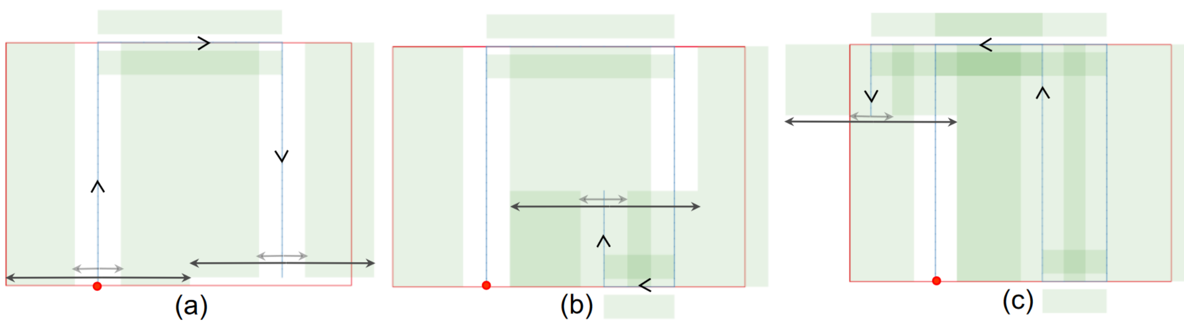

Figure 4.3: Illustration of an in-progress Return (Vertical) strategy performed by a single AUV with blind zone.

Another way we could approach the gaps left out by original zigzag strategies (for ex: Horizontal) is to perform a return trip in a similar fashion hopefully covering all the remaining gaps. On either end of the footprint, $dS - dB$ is covered while dB is left out. Hence, a single return trip would be sufficient if $dS - dB \geq dB \Rightarrow dS \geq 2 \cdot dB$. Otherwise, multiple forward and return trips would be required to achieve full coverage. We show an illustration of this strategy in Fig. 4.3 with a blind-zone AUV performing vertical zigzag motion.

Corollary. `Return` *strategy achieves full coverage of* $\mathcal{R}$ *when* $dS \geq 3 \cdot dB$.

4.3.5 Complete Zigzag

We now present a strategy which we name `Complete Zigzag` (`CZ`) and it is same as the pair of lines method in (Hagen, 2011) or the maximum area coverage method in (Hagen and Hansen, 2007). This method underpins most of the strategies we develop later on for multiple AUVs as they use the same path (waypoints) generated by `Complete Zigzag` for exploring the desired region $\mathcal{R}$ while optimizing how to partition and assign the different parts to each vehicle. We provide a formal proof of its coverage

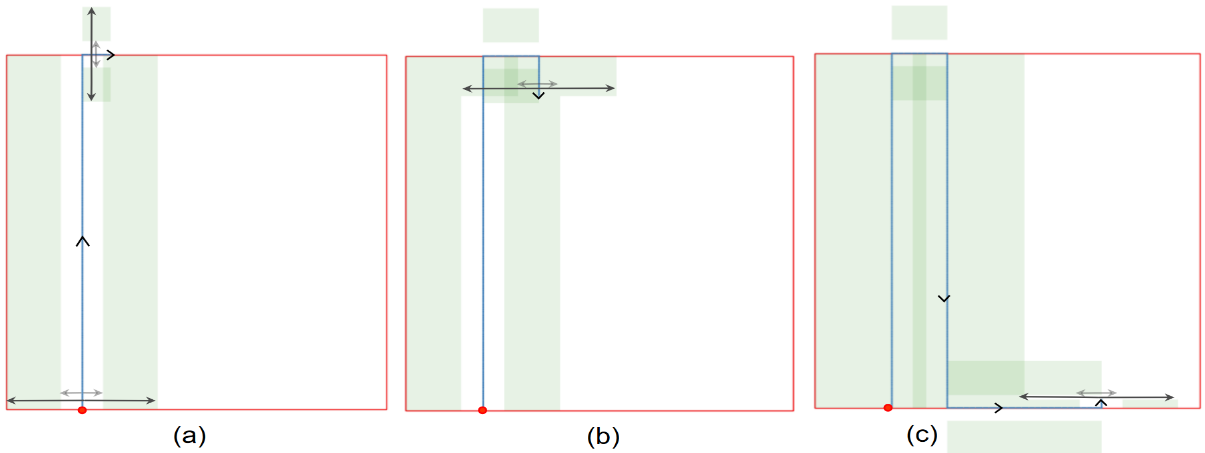

Figure 4.4: Illustration of an in-progress Complete Zigzag strategy performed by a single AUV with blind zone.

which will also act as the basis for the theoretical guarantees of the methods we develop later for multiple AUVs.

In this strategy, the sensor footprints are used in a complementary fashion by covering the gaps left in the forward motion during the backward motion. We place the AUV initially at $(dS, 0)$ so that its left footprint reaches the left end of $\mathcal{R}$. The AUV ascends vertically to the other side, then turns and moves perpendicularly until its right footprint occurs at the place where its left blind zone was present earlier. Descending vertically, a rectangular strip is covered possibly with overlap. By repeating this back-and-forth motion, the AUV can cover its own nadir gap while returning, ultimately encompassing the entire `AoI`. An illustration of an AUV executing `CZ` motion is is shown in Fig. 4.4. We note that there may be cases where the right footprint does not fully cover gap left during forward motion, so we establish `CZ`'s coverage property next.

Theorem 1. *`CZ` strategy achieves full coverage of $\mathcal{R}$ when $dS \geq 3 \cdot dB$.*

Proof. First, transport the AUV from its starting location initially to the coordinate $(dS, 0)$ so that the left footprint can reach till the end of the nearest side of the rectangle. We then send it vertically upwards to the other side reaching the coordinate (dS, B) (Fig.4.4(a)). We notice that the area between the lines $y = dS - dB$ and $y = dS + dB$ is left out while everything to the left of $y = dS - dB$ is covered. Hence, to begin coverage from $y = dS - dB$ line next, we require the AUV's right sensor footprint (coming down vertically now) to reach that line. Thus, the AUV is turned and moved from (dS, B) till $\big((dS - dB) + dS, B\big) = \big(2 \cdot (dS - dB), B\big)$ (Fig.4.4(b)). Now, the right footprint extends from $y = dS - dB$ to $y = dS - dB + (dS - dB) = 2 \cdot (dS - dB)$. Recall that the region left out was between the lines $y = dS - dB$ to $y = dS + dB$ which can now (coming back to complete the current trip) be covered *entirely* if

$$2 \cdot (dS - dB) \geq dS + dB$$
$$\Rightarrow dS \geq 3 \cdot dB$$

Once, the AUV has come down and reached $x = 0$ line, an entire strip of size $(3 \cdot dS - dB) \times B$ is covered with an overlap of size $(dS - 3 \cdot dB) \times B$. We can consider the remaining rectangle as a new problem with reduced dimension (Fig.4.4(c)) and keep simulating the AUV to cover a complete strip of $\mathcal{R}$ in each trip until the whole AOI is explored. $\square$

4.4 Theoretically Analyzing Overlap

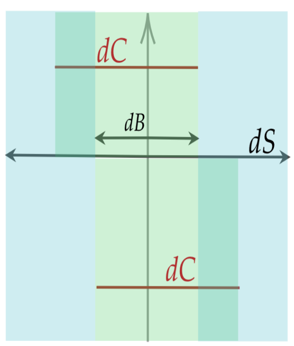

(a) When the AUV travels through an already explored area such that blind zones don't result in any gaps.

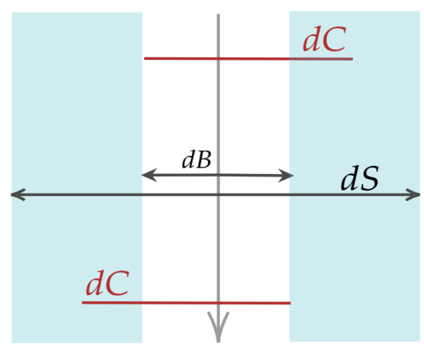

(b) When the AUV travels through (partially) unexplored area leaving gaps. Here, maximal gap of size $2 \cdot dB$ is shown though any non-zero gap could be possible.

Figure 4.5: Coverage footprint (shown in light blue strips) of a single AUV with blind zone with possible trajectory shown in grey. Light green strips denote already explored areas while darker regions denote current area under overlap. The white strips represent the area not explored by the AUV. Here, dC represents the length of area (a) already covered or (b) will be covered in the future by the AUV.

Here, we try to briefly reason about the least amount of overlap that has to be incurred by an optimal strategy (one which achieves full coverage) to better understand the performance of the strategies we developed earlier. Let `Opt` be such an optimal strategy. We conjecture the following regarding the `Complete Zigzag` (`CZ`) strategy:

Conjecture. *`CZ` strategy achieves minimal overlap (i.e, not more than `Opt`).*

Rationale. Let us analyze a point $P = (x, y)$ of its trajectory which is inside $\mathcal{R}$. Also let $dC = dS - dB$ be the length of the strip of area covered any moment. When the AUV is at P (assuming travelling in vertical direction for simplicity[1]), there are two possible cases of the effect of blind-zone:

[1] Our analysis can be extended to any direction of motion from P

1. Blind-zone doesn't result in any gap due to the fact that the region $(x - dB, x + dB)$ was already explored by the AUV earlier (Fig. 4.5a). In such a case, a strip of length dC subsumes the interval $(x - dB, x + dB)$. However, rest of the portion of dC must lead to overlap as it is contained in the span of the AUV's footprint: $(x - dS, x + dS)$. Therefore, the following amount of overlap will occur at the least:
$$dC - 2 \cdot dB = dS - 3 \cdot dB$$
2. Blind-zone results in non-zero gap (Fig. 4.5b). In such a case to achieve full coverage, the AUV must come near P sometime in the future so that its sensor footprint covers this gap. Hence, an overlap will incur at that moment and it will be minimal if this gap is maximal. The maximal gap possible to leave at any moment is $2 \cdot dB$ thus the minimal overlap is
$$dC - 2 \cdot dB = dS - 3 \cdot dB$$

Thus, through our informal case analysis, we observe that $dS - 3 \cdot dB$ lengths of strip will be part of overlap of `Opt`. The only remaining part is the way in which the trajectory of `Opt` covers $\mathcal{R}$. If there was no blind-zone, we know zig-zag strategy would be optimal (horizontal/vertical). As `CZ` is zig-zag inherently and incurs an overlap of size $(dS - 3 \cdot dB) \times B$ in one trip (back and forth), we end with our hypothesis that `CZ` achieves minimal overlap (i.e, not more than `Opt`).

4.5 Simulation Results

We now simulate the different strategies proposed earlier for single AUV coverage path planning to evaluate their performance. We use the evaluation setup mentioned in Section 3.4. Given our primary interest is in *complete* coverage of $\mathcal{R}$, so we compare `No Gaps` (Section 4.3.3), `Return` (Section 4.3.4) and `CZ` (Section 4.3.5) on the different input settings discussed earlier (Section 3.4), as all of them achieve 100% coverage under the characteristics of our problem formulation [2]. We show the performance of these strategies (via line plots) for the metrics *overlap, distance* and *turns* in Figures 4.6 and 4.7.

4.5.1 Lower Bound

To put the performance of these strategies in perspective, we use the basic zigzag (vertical/horizontal depending on the orientation of $\mathcal{R}$) with gaps as a lower bound. We can think of this strategy as treating dB to be 0, and since there are no obstacles in $\mathcal{R}$, its coverage pattern and consequently, its results on the different metrics (shown via dashed red line in Figures 4.6 and 4.7) act as a valid lower bound for any *complete* strategy.

[2] ie., $dS \gg dB$.

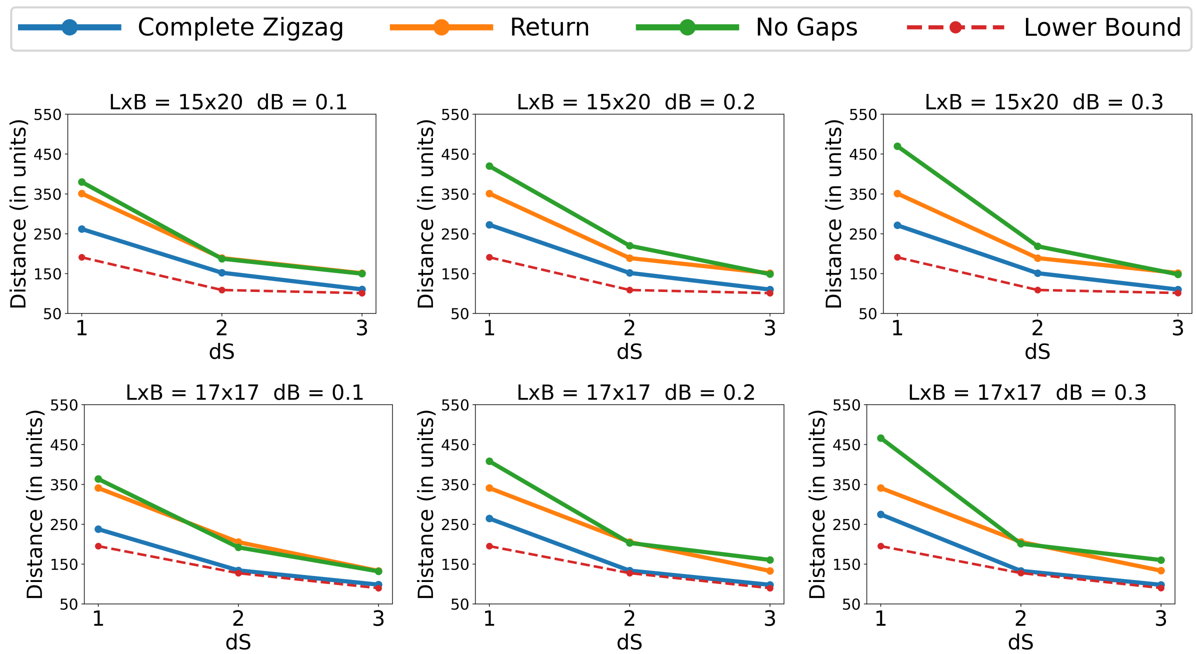

Figure 4.6: Line plots denoting the *distance travelled* by the AUV in different strategies for varying values of dS and dB on the two different input configurations (rectangle and square).

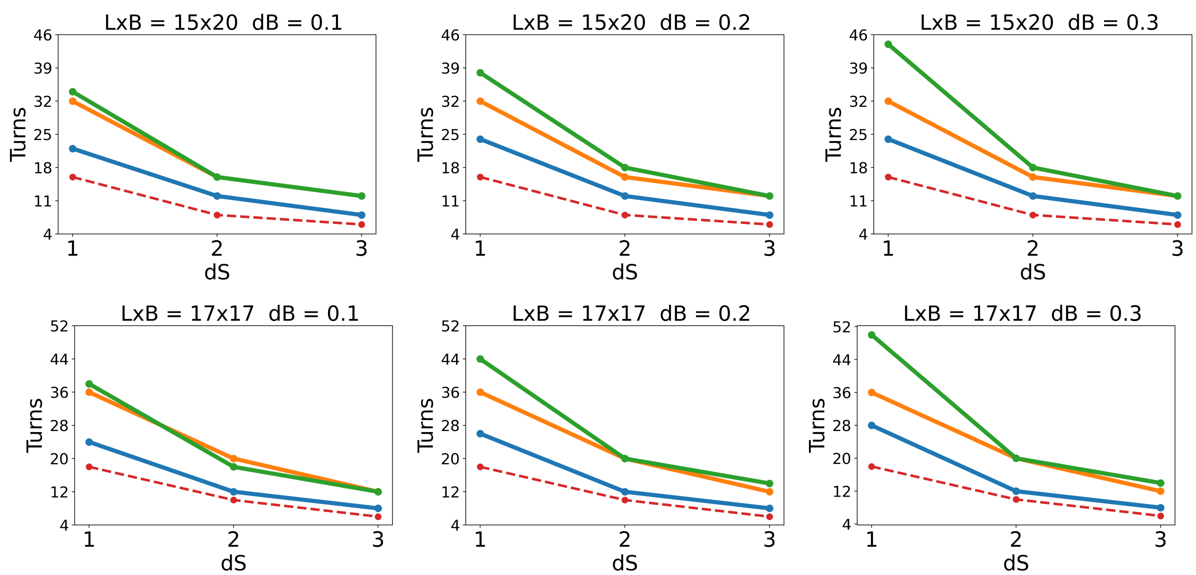

Figure 4.7: Line plots denoting the *number of turns taken* by the AUV in different strategies for varying values of dS and dB on the two different input configurations (rectangle and square).

4.5.2 Discussion

The relative performance of the different strategies was found to be consistent in both the environments (rectangle of dimension 15×20 units and square of dimension 17×17 units) across all the metrics considered and also over the different values of dS, dB considered.

We see a clear distinction in the performance of the different strategies with `Complete Zigzag` (`CZ`) being the best across *both* of our metrics followed by `Return` and `No Gaps` respectively. `CZ` achieves significantly lower values than the other two strategies in each of the metric. As one might expect, increasing the sensor coverage range (dS) while keeping the nadir gap fixed (dB) leads to less distance and lower number of turns which we observe in the plots (Figures 4.6 and 4.7). Also, increasing the size of the nadir gap while keeping the width of the sensor swath fixed seems to have an adverse effect for `No Gaps` strategy as its performance deteriorates with increase in nadir gap which doesn't happen for `Return` and `CZ`.

In terms of both distance and number of turns, `CZ` sometimes is quite close to the lower bound, especially with higher values of dS, hinting it may be the optimal strategy for a single AUV with nadir gap. For example, at $dS = 3$, the distance travelled by the AUV following `Complete Zigzag` strategy is almost same as the lower bound. We had given a rationale for its potential optimality (in terms of overlap) in Section 4.4.

Overall, we find `Complete Zigzag` to be the best strategy. Both our theoretical and empirical findings provide additional support to the reason why `Complete Zigzag` strategy is used in practice for exploration with single AUV with nadir gap (Hagen and Hansen, 2007; Hagen, 2011).

Chapter 5

Exploration with two AUVs

5.1 Motivation

In this chapter, we explore the complexities of coverage path planning (CPP) with two Autonomous Underwater Vehicles (AUVs), focusing on overcoming the challenges posed by nadir gaps or blind zones. Addressing the challenge of nadir gap and cooperation with two AUVs not only provides insights into effective path planning but also introduces the foundational elements for coordinating multiple AUVs in CPP tasks.

The use of two AUVs offers a unique opportunity to examine the dynamics of collaborative exploration and the potential for enhanced coverage efficiency. Despite the increased complexity, this scenario allows for innovative approaches to minimize mission completion time through strategic vehicle placement and movement synchronization. The main objectives include developing algorithms that enable the AUVs to achieve full coverage while dividing the workload effectively to minimize completion time, and setting the stage for multi-AUV coordination.

5.2 Problem Formulation

In this chapter, we are interested in the coverage of planar underwater environments using two AUVs with nadir gaps. We define our problem of *offline* exploration in two-dimensional environment using the following tuple $\langle \mathcal{R}, N, \mathcal{S}, v, dS, dB \rangle$:

- $\mathcal{R}$ denotes the rectangular `AoI` of size $L \times B$ in the global frame whole of which needs to be covered once.
- N is the number of AUVs available for planning. Here, $N = 2$.
- $\mathcal{S}$ is the list of AUV deployment locations where $\mathcal{S}_i$ is a tuple (x_i, y_i) denoting the starting and returning coordinate for the i^{th} AUV. The size of $\mathcal{S}$ is 2 in this case.
- v is the (constant) speed at which each AUV travels.

- dS is the length of sensor footprint covered by the vehicle perpendicular to its direction of motion. We model it as a scalar quantity on both sides of the motion (Fig. 3.1b).

- dB denotes the distance of blind zone left by the vehicle perpendicular to its direction of motion, modelled similarly as dS (Fig. 3.1b).

Our primary objective is to ***(a)*** *achieve* ***complete*** *coverage of the area of interest (*`AoI`*)* while our secondary objectives are either ***(b)*** *minimizing the maximum distance travelled by any of the AUVs* or ***(c)*** *minimize the total number of turns made by the AUVs*. Note that each (secondary) objective represents a distinct aspect of the mission, and *optimizing for one may compromise the other* (Yordanova et al., 2019). Thus, there may not be a single strategy optimal across all the objectives. Thus, we develop strategies tailored for each objective and empirically analyze their performance.

5.3 Strategies

Now that we have more than one AUV, we would like to divide the plan such that overall time to cover $\mathcal{R}$ completely is minimized. We first introduce below a novel technique to cooperatively use both the AUVs and also discuss how to extend past single-AUV strategies for two AUVs.

5.3.1 Multi-Zigzag

One way we could try to cover the blind-zone of a AUV is to use the second AUV such that both can cover each other's blind zones. By placing these AUVs consecutively (on one side of $\mathcal{R}$ such that all of them move perpendicularly to the other side), the first AUV's right sensor footprint can hopefully cover the blind zone of the second AUV (and vice versa for the first AUV) and together they can travel leaving no gaps. We can think of this arrangement as one global AUV with no blind zone having much larger sensor footprint (possibly with overlap) with which we can perform a simple zigzag motion to achieve full coverage. We refer to this strategy as `MZ`. However, it is also possible that if the blind zone takes up a significant portion of the sensor footprint, then each AUV may not be able to fully cover the blind-zone of its nearby AUVs. We formalize this property below.

Theorem 2. *`MZ` strategy achieves full coverage of $\mathcal{R}$ (requiring at least 2 AUVs) if $dS \geq 3 \cdot dB$.*

Proof. Let us place the first AUV at $(dS, 0)$ so that its left footprint can cover the bottom-left corner $(0, 0)$. Now, to cover its blind zone which ranges from $[dS - dB, dS + dB]$, we would have to place the second AUV at such a place so that its left sensor footprint reaches the left blind-zone of the first AUV. Thus, the second AUV's initial x-coordinate is $(dS - dB) + dS = 2 \cdot dS - dB$. Meanwhile, the right footprint of first AUV covers the region $[dS + dB, 2 \cdot dS]$ while the left footprint of second AUV covers

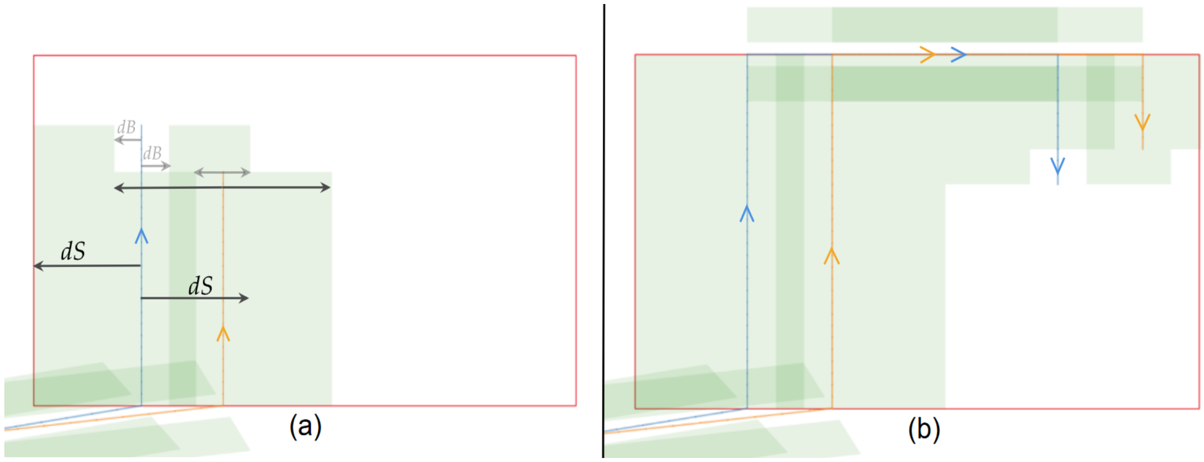

Figure 5.1: Illustration of an in-progress Multi Zigzag strategy performed by two AUVs with blind zone.

the region $[2 \cdot dS - dB, 2 \cdot (dS - dB)]$ horizontally. The second AUV can cover the right blind zone of first AUV and vice versa for the second AUV if $2 \cdot (dS - dB) \geq dS + dB \Rightarrow dS \geq 3 \cdot dB$.

As the AUVs move vertically and reach the other end, we notice that an entire rectangular strip of size $3 \cdot dS - dB \times B$ is covered with an overlap of size $(dS - 3 \cdot dB) \times B$. Thus, we can consider the remaining rectangle as a new problem with reduced dimension and simulate the AUVs like initially done from the other end. $\square$

5.3.2 Complete Zigzag with Two AUVs

In our empirical evaluations for a single AUV (Section 4.5), we found that `CZ` strategy emerged as the best approach in terms of both distance travelled and turns performed. Given its promising performance, extending `CZ` for two (and eventually multiple) AUVs is a logical next step, and we refer to this extension of `Complete Zigzag` for two AUVs as $\texttt{CZ}_2$.

Let P be the path obtained from `CZ` strategy for a single AUV. Note that the starting point of P may be different from $\mathcal{S}_1$. Hence, the AUV has to reach the starting point of P and also return back to $\mathcal{S}_1$ from the last point of P.

To extend `CZ` to $\texttt{CZ}_2$, we divide the path P obtained from `CZ` (for a single AUV) into approximately equal parts (P_1 and P_2) to be executed independently by a different AUV. As the line-segments joining the waypoints in P do not intersect with themselves, so no explicit coordination between AUVs is required. However, by just dividing P as equally as possible, notice that the starting point of P_1 is near $\mathcal{S}_1$ unlike the starting point of P_2 which is far off from $\mathcal{S}_2$ (Fig.5.2 (a)). Consequently, the second AUV has to travel a longer distance both while going and returning to cover its part P_2. This leads to first AUV completing its work much earlier than the second AUV, so the second AUV does a greater amount of work compared to first AUV. Thus, we observe that equal division of P actually leads to unfair division

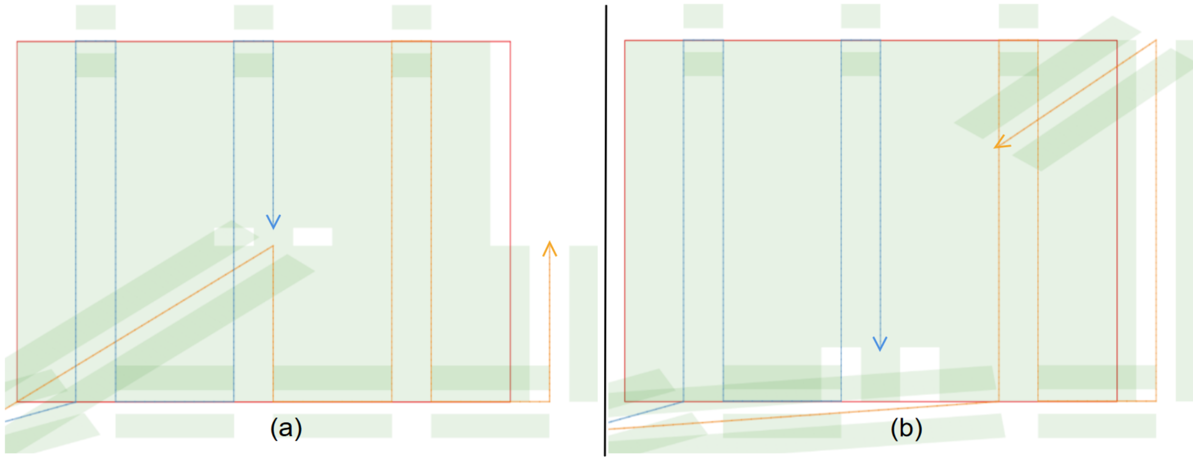

Figure 5.2: Illustration of in-progress Complete Zigzag (CZ) strategy for two AUVs with blind zone with (a) near equal division of the global path generated by CZ leading to large difference in completion times of the AUVs (b) near equal division for the work (by unequal division of the path) to be undertaken by each AUV to minimize the overall completion time.

of work. Ideally, we would like to finish coverage of $\mathcal{R}$ in least time possible so the maximum work done by any AUV should be minimized.

To achieve the above objective, we can iterate over the waypoints of P and check whether the current waypoint is optimal for dividing P. At each waypoint, for both the AUVs, we will have calculate the distance in their subpath P_i while also taking into account the distance from their starting location $\mathcal{S}_i$ to the beginning point of P_i and also the distance while returning from the last location in P_i to $\mathcal{S}_i$. The waypoint in P which results in minimum distance among the maximum of the two AUVs is optimal for division. An example of such a division of P is shown in Fig. 5.2 (b).

5.3.3 Turn-Aware Zigzag

While the above way of extending `Complete Zigzag` (`CZ`) is a promising way to fruitfully use all the vehicles, a potential drawback of the above approach is the likely increase in number of turns.

Let P be the path obtained from `CZ` strategy for a single AUV and P_1, P_2 be the paths obtained by $\texttt{CZ}_2$. Notice that if the end-point of P_1 (or the start-point of P_2, since they are the same) is not a turning point in the original path P, then the first vehicle will have to execute a (extra) turn as it has to change its direction to return to $\mathcal{S}_1$; similarly, for the second AUV to begin its work. An example of this is shown in Fig. 5.3(a).

Thus, when the primary objective is to minimize the number of total turns, `CZ` may not be optimal. However, we can tweak how we partition P for two AUVs such that the total number of turns incurred by them is not more than the number of turns caused while `CZ` is executed by a single AUV. We describe the below such a strategy and name it $\texttt{TZ}_2$ (`Turn-aware Zigzag`, specifically for two AUVs).

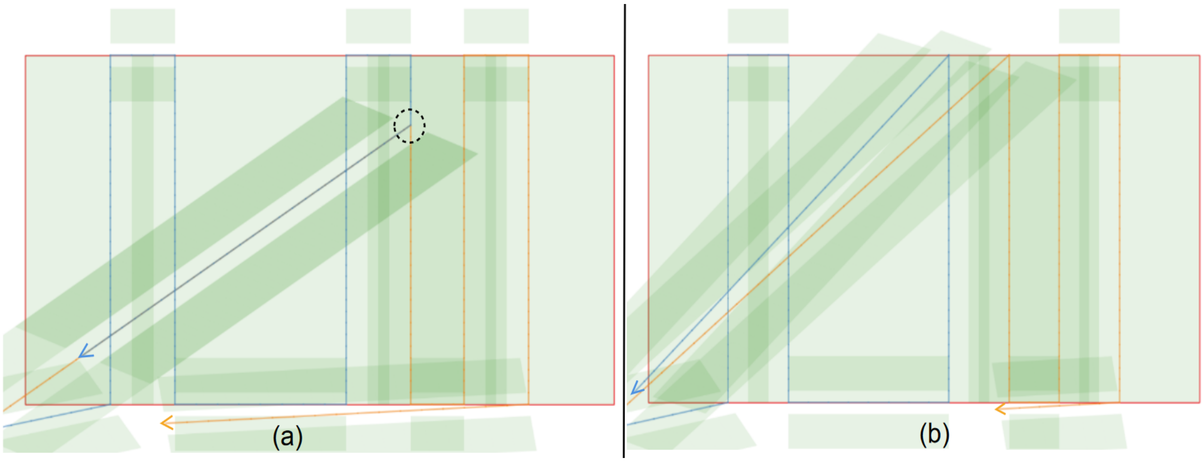

Figure 5.3: Illustration of number of turns taken by (a) $\texttt{CZ}_2$ and (b) $\texttt{TZ}_2$. The dashed black circle signifies the returning (starting) location for the first (second) AUV. As this waypoint doesn't coincide with an already turning point in the original (one vehicle) CZ strategy, so this **causes** 2 **extra turns**.

In $\texttt{TZ}_2$, we *only consider those waypoints in P, for division, where a turn occurred in the original strategy CZ*. Dividing P at any such waypoint will partition it into two subpaths P_1 and P_2 and we choose that waypoint which minimize the maximum distance any AUV will have to travel taking into account the overhead of the distance to and fro from its starting location. This ensures that $\texttt{TZ}_2$ achieves a Pareto-optimal solution in terms of the total number of turns made by the AUVs and the completion time for entire exploration.

Corollary. *$\texttt{TZ}_2$ for two AUVs incurs the same number of total turns as CZ for one AUV.*

5.3.4 Extending Other Past Strategies

Similar to how we extended CZ for two AUVs, we can generalize that scheme to any single AUV strategy – take the path generated by the given technique, divide it into N parts such that each part is executed by a specific AUV simultaneously.

For the Return strategy we defined in previous section, this would imply that the first AUV does *only* the forward exploration leaving gaps while the second AUV executes *only* the return journey. However, an important aspect to be considered is that no collision should occur while each AUV independently follows its path as both are traversing in opposite directions. Meanwhile, the No Gaps method can be extended in a fashion exactly same as we extended CZ for two vehicles. Here, as the paths for the AUVs do not intersect with one another or itself and the both the AUVs travel in same direction but at a distance apart, so no explicit coordination between AUVs is required to handle collision.

5.4 Simulation Results for Two-AUV Strategies

We now simulate the different strategies proposed earlier for coverage path planning with two AUVs to evaluate their performance. We use the evaluation setup mentioned in Section 3.4. Given our primary metric of interest is the target area explored (*coverage*), we skip extending `Return` and `No Gaps` for two vehicles given their poor performance for single vehicle, especially incomplete coverage[1] (Section 4.5). We rather focus our attention to the newly developed algorithms, i.e., Multi-Zigzag ($\mathtt{MZ}_2$), Turn-aware Zigzag ($\mathtt{TZ}_2$) and Complete Zigzag for two vehicles ($\mathtt{CZ}_2$).

To evaluate the performance of these strategies, we perform simulations on different input parameters following *exactly* the same setup as described earlier in Section 5, unless mentioned otherwise below. While the input area (of size $L \times B$) was represented from coordinates $(0, 0)$ to (L, B), the starting and returning location for the AUVs were the following:

1. (-8, -5) for the first AUV.

2. (-3, -5) for the second AUV.

Given that all the strategies being evaluated ($\mathtt{MZ}_2$, $\mathtt{TZ}_2$, $\mathtt{CZ}_2$) achieve full coverage under their required assumptions[2], we skip plotting their coverage percentage and showcase their performance on other relevant metrics. Specifically, we measure the maximum distance travelled by any of the AUVs (which essentially determines the completion time of the mission), total number of turns performed cumulatively by the AUVs and the overlap incurred[3]. The performance of the strategies on these metrics is shown in Fig. 5.4 and Fig. 5.5.

5.5 Discussion

The relative performance of the different strategies was found to be consistent across the environments (rectangle of dimension 15×20 units and square of dimension 17×17 units) and the different values of dS, dB considered. For each metric, we see a clear distinction in the performance of the strategies though the relative difference between the strategies is not as high as we saw in the case of single AUV (Figures 4.6 and 4.7). We discuss the performance of strategies on each of the considered metrics below:

- *Maximum Distance:* We find that `Complete Zigzag` ($\mathtt{CZ}_2$) achieve the lowest maximum distance, closely followed by $\mathtt{TZ}_2$ and $\mathtt{MZ}_2$. This is expected as $\mathtt{CZ}_2$ is designed to minimize the maximum distance travelled by any vehicles by incorporating distance from their starting (returning) locations into their coverage trajectories.

[1]Note that their (naive) extension for two vehicles will also not achieve full coverage.
[2]which is satisfied in our setup.
[3]More discussion about these metrics has been done earlier in Section 3.4.

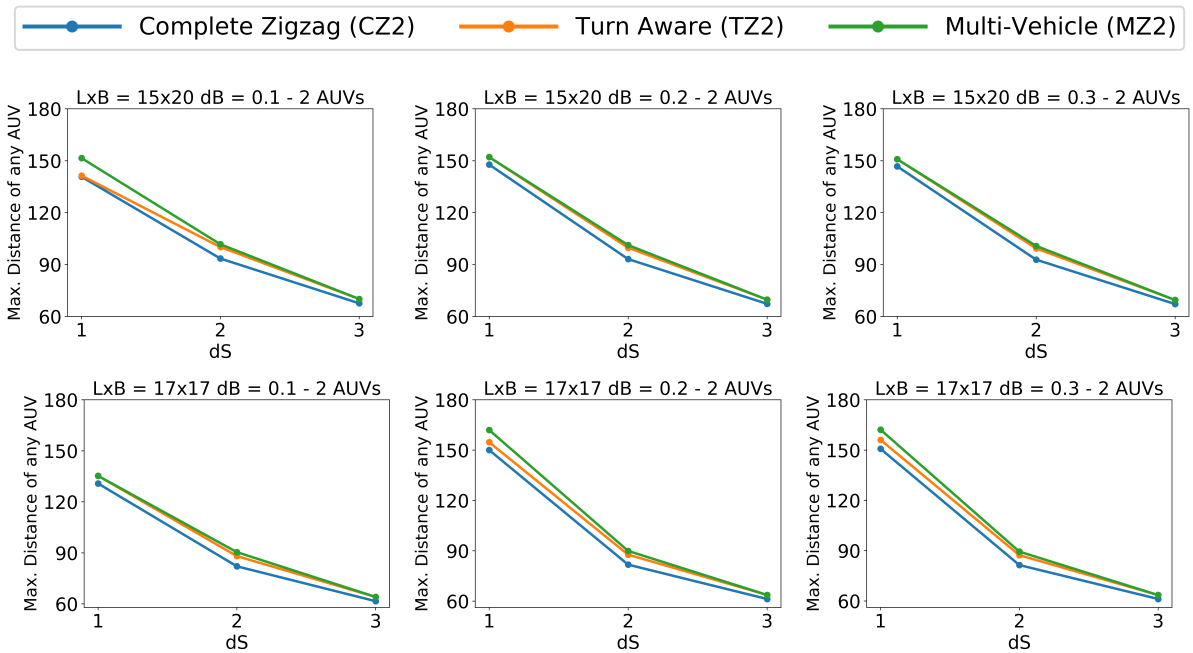

Figure 5.4: Line plots denoting the **maximum distance travelled by any of the two AUVs** in different strategies for varying values of dS and dB on the two different input configurations (rectangle and square).

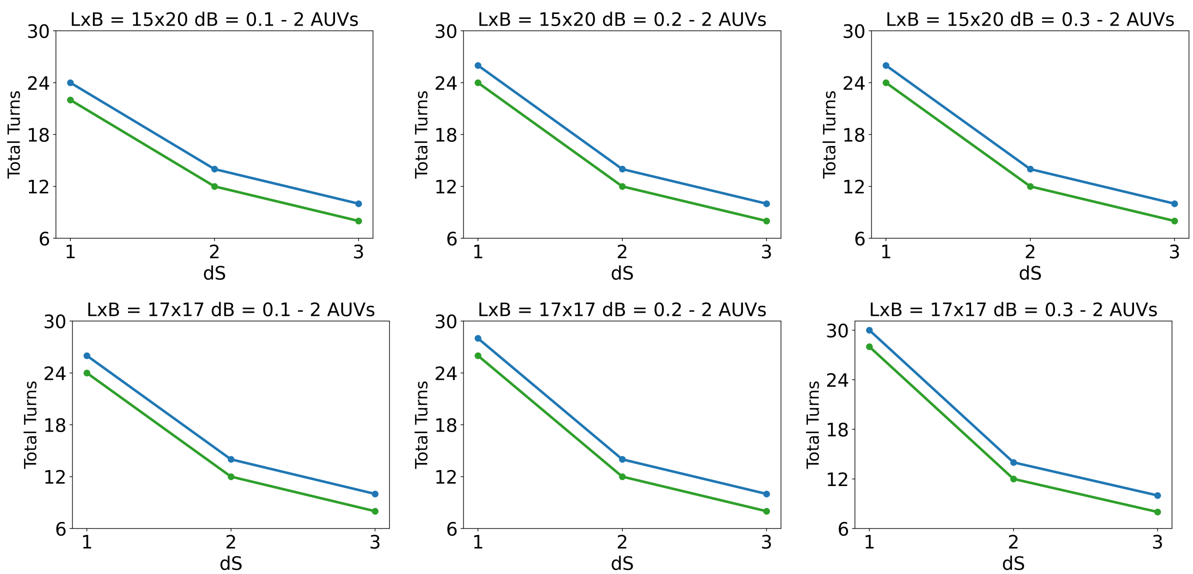

Figure 5.5: Line plots denoting the **total number of turns taken** by the two AUVs in different strategies for varying values of dS and dB on the two different input configurations (rectangle and square). *Please note that the yellow line ($\mathtt{TZ}_2$) is invisible for the above plots as it is same as the green line ($\mathtt{MZ}_2$) which has been plotted on top of it.*

- *Turns:* We find that $\texttt{TZ}_2$ and $\texttt{MZ}_2$ achieve the lowest number of (total) turns, closely followed by $\texttt{CZ}_2$. Given that the actual coverage trajectory of both $\texttt{TZ}_2$ and $\texttt{MZ}_2$ (upon taking union of each AUV's individual trajectory) has the same waypoints for turning as in the path generated by $\texttt{CZ}$ for one AUV, it is not surprising that they achieve the lowest number of turns. Regarding $\texttt{CZ}_2$ resulting in more turns, we had noticed earlier that it might incur two more turns per (each) AUV as shown in Fig. 5.3.

Overall, we find that the best strategy would depend on the use case. If we plan to minimize the total number of turns, $\texttt{TZ}_2$ and $\texttt{MZ}_2$ are the most promising strategies. If the cost of turning is not significant and minimizing maximum time spent by any vehicle is the primary objective, then $\texttt{CZ}_2$ would be the best strategy.

Chapter 6

Failure-Aware Exploration with two AUVs

In this chapter, we extend our study on coverage path planning (CPP) to scenarios involving two Autonomous Underwater Vehicles (AUVs) with nadir gaps, focusing on addressing the challenge posed by the *potential failure of one AUV*. The capability of handling such dynamic and realistic scenarios is crucial, as it introduces the need for on-the-fly adaptation to ensure complete area coverage despite unforeseen AUV failures.

The possibility that one AUV might fail arbitrarily demands robust and flexible planning algorithms capable of quickly reallocating coverage responsibilities to the other operational AUV to fill in the coverage gaps and region left unexplored by its counterpart. It not only tests the resilience and adaptability of the CPP strategy but also the efficiency with which the second AUV can recalibrate its mission to cover the originally planned area of the first AUV, in addition to its own assigned region.

The motivation for exploring CPP with two AUVs under the risk of failure is to develop a deeper understanding of multi-AUV coordination, redundancy planning, and real-time mission adaptation. This setup aims to ensure complete coverage minimizing the distance or the number of turns performed under partial system failures, thereby setting the groundwork for more complex multi-AUV operations that can withstand individual vehicle failures without compromising the overall mission objectives.

6.1 Problem Formulation

In this chapter, we are interested in the coverage of planar underwater environments using two AUVs with nadir gaps where *one of them might fail (die) unexpectedly*. Thus, our problem is of *online* exploration in two-dimensional environment as the input for AUV failure arrives real-time. We define our problem using the following tuple $\langle \mathcal{R}, N, \mathcal{S}, v, dS, dB, (j, t)\rangle$:

- $\mathcal{R}$ denotes the rectangular `AoI` of size $L \times B$ in the global frame whole of which needs to be covered once.
- N is the number of AUVs available for planning. Here, $N = 2$.

- $\mathcal{S}$ is the list of AUV deployment locations where $\mathcal{S}_i$ is a tuple (x_i, y_i) denoting the starting and returning coordinate for the i^{th} AUV. The size of $\mathcal{S}$ is 2 in this case.
- v is the (constant) speed at which each AUV travels.
- dS is the length of sensor footprint covered by the vehicle perpendicular to its direction of motion. We model it as a scalar quantity on both sides of the motion (Fig. 3.1b).
- dB denotes the distance of blind zone left by the vehicle perpendicular to its direction of motion, modelled similarly as dS (Fig. 3.1b).
- (j, t) denotes the real-time control input received arbitrarily during execution where j denotes the AUV which failed at the timestamp t. *Note that this input is optional and may not be received in the case of no failures.*

The goal is to re-plan the path for the other AUV j' such that complete coverage of $\mathcal{R}$ is achieved by the end of the mission. More specifically, our primary objective is to ***(a)*** *achieve* ***complete*** *coverage of the area of interest (*`AoI`*)* while our secondary objectives are either ***(b)*** *minimizing the maximum distance travelled by any of the AUVs* or ***(c)*** *minimize the total number of turns made by the AUVs*.

6.2 Strategies for Robust Planning

We now discuss how to extend the each of the strategies developed in the previous chapter for two AUVs to account for the failure of one of the AUVs.

6.2.1 Robust Complete Zigzag for Two AUVs

Recall that `Complete Zigzag` for two AUVs partitions the trajectory by `CZ` for one AUV such that the maximum distance travelled by any AUV is minimized (consequently, minimizing the overall mission completion time). Thus, both AUVs follow a subpart of the original trajectory. One simple way to handle failures is for r' to reach the location where r failed, after completing its own trajectory, and continuing r's remaining path. Given that the original strategy had complete coverage, this extension also offers complete coverage.

Actually, there is a better way to handle failures when following `CZ` strategy exploiting the fact that we have an even number of AUVs for operation. Recall that both the AUVs travel in the same direction when following `CZ`. Notice that if the first AUV fails, the second AUV has to take a turn and come back to the location of failure of the first AUV and complete its remaining path. However, if the second AUV were to follow its planned trajectory in reverse manner, that is start from its end-point and finish at its starting-point, then it can simply continue from the new end-point (which was its original start-point but also the end-point for first AUV) to the location of failure of the first AUV. This would not incur the extra distance required to explicitly reach the spot of failure because that distance is now being fruitfully used to cover $\mathcal{R}$ by following the remaining trajectory of r in reverse manner. An example of this is shown in. Here, both the AUVs simultaneously explore $\mathcal{R}$ in a diagonally opposite manner so that additional work (distance and possibly, turns) due to failure is minimized. We refer to this modified strategy as `Robust Partition Zigzag` Robust $\mathtt{PZ}_2$.

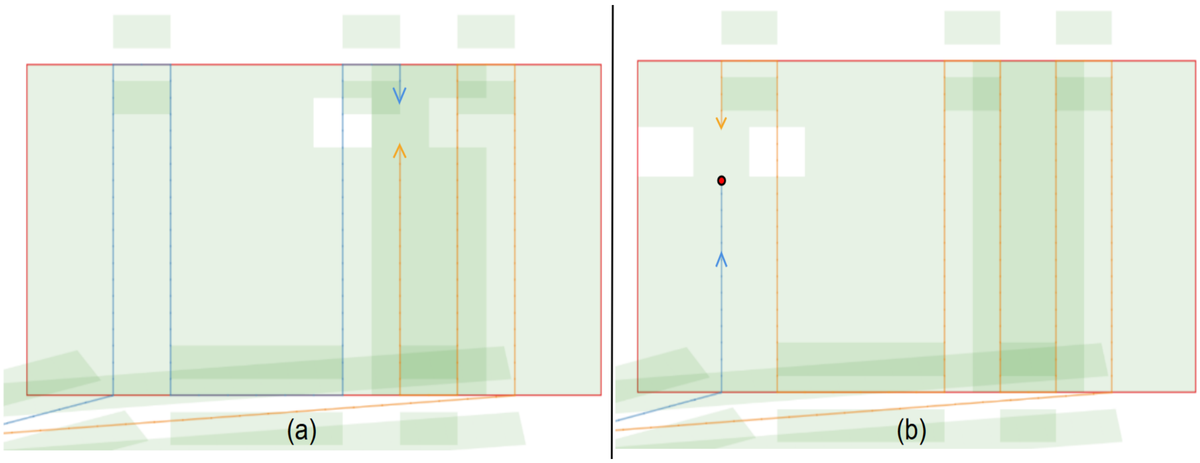

Figure 6.1: (a) Illustration of `Complete Zigzag` ($\mathtt{CZ}_2$) strategy with the second AUV following its trajectory in reverse manner. (b) Illustration of Robust $\mathtt{PZ}_2$ where the first AUV fails early (highlighted by red dot with black boundary) and the second AUV continues after finishing its own trajectory until it reaches the failure location (from where it would return).

6.2.2 Robust Turn-Aware Zigzag for Two AUVs

Similar to how we have extended `Complete Zigzag` (CZ) for two AUVs with failure above, we can likewise extend `Turn-Aware Zigzag` by making the second AUV follow its trajectory in reverse manner and let r' simply continue after its end-point as the failure location of r will lie in its additional path and no directional change would be required. We refer to this modified strategy as Robust $\mathtt{TZ}_2$.

6.2.3 Robust Multi-Zigzag for Two AUVs

Recall that in `Multi-Zigzag`, we place both the AUVs consecutively such that the first AUV's right sensor footprint covers the blind zone of the second AUV[1] (and vice versa for the first AUV) and together they travel leaving no gaps. Here, both the AUVs enter $\mathcal{R}$ near one another (as they have to cover each other's blind zone) and also both of their end-point in $\mathcal{R}$ is in close vicinity. Thus, what we can do is let e' do its work and after finishing its trajectory, it should go to the end-point of r and execute r's trajectory in reverse manner until it reaches the location of failure from where it can return. This way, the additional distance incurred to start useful work is minimized as both their end-points in $\mathcal{R}$ are

[1]Assuming $dS \geq 3 \cdot dB$.

close by so the healthy AUV r' has to travel only a small distance to resume useful work (of covering $\mathcal{R}$. We refer to this modified strategy as $\texttt{Robust MZ}_2$.

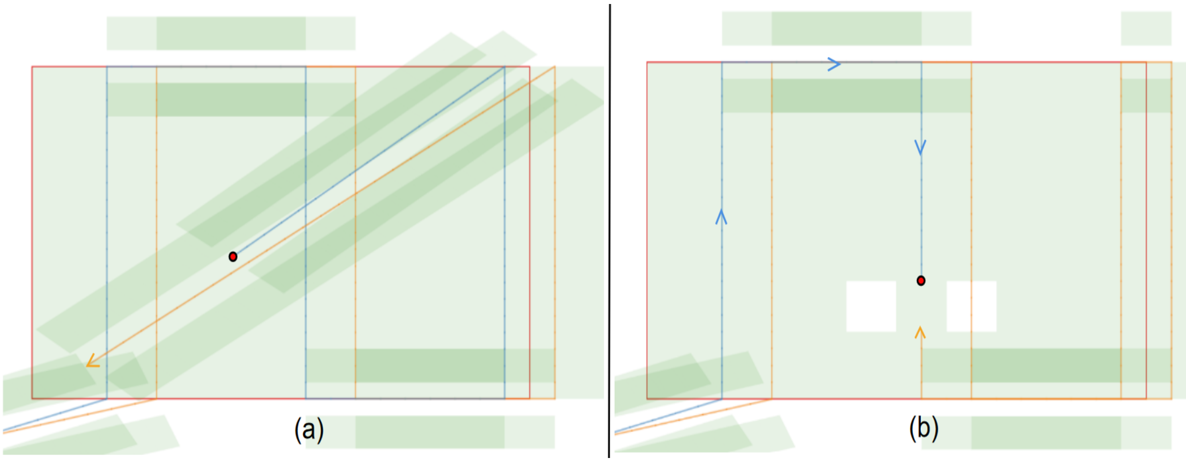

Figure 6.2: (a) Illustration of $\texttt{Robust TZ}_2$ where the first AUV fails while returning (after completing its assigned task). (b) Another illustration of $\texttt{Robust TZ}_2$ where the first AUV fails early (highlighted by red dot with black boundary) and the second AUV follows the trajectory of the first AUV from the end (after completing its own trajectory) until it reaches the failure location (from where it would return).

6.3 Results for Strategies developed for Two AUVs *with Failures*

6.3.1 Setup

To compare the robustness of the different strategies developed for handling two AUVs with failure, we first need to come up with a proper method for evaluation. In reality, it is possible that a vehicle may fail arbitrarily during its trajectory (unless we have more knowledge about the input parameters and the environment for deployment). To capture this arbitrariness, we can use randomization and repeat the experiment a significant number of times to get an estimate of the performance of the strategies.

To implement the above idea, before starting an experiment, we randomly chose one of the two vehicles (say i) and one of the waypoints from its trajectory which will be the point of failure (say p). After these parameters are fixed, we let the strategy run until the AUV i reaches point p at which we inform the strategy of the failure on the fly. The strategy returns new trajectories for both the AUVs which is then followed. Apart from this, we follow exactly the same setup and input configurations described earlier (in Section 3.4), evaluating the strategies on total number of turns and maximum distance travelled by any vehicle.

We ran each experiment for 1000 trials to get a distribution of values for each metric and we plot the *mean* value along with the standard error as bar plots shown in Fig. 6.3 and 6.4. To get more insight into these values, we can compare them with their non-failure counterpart. Each robust strategy has a

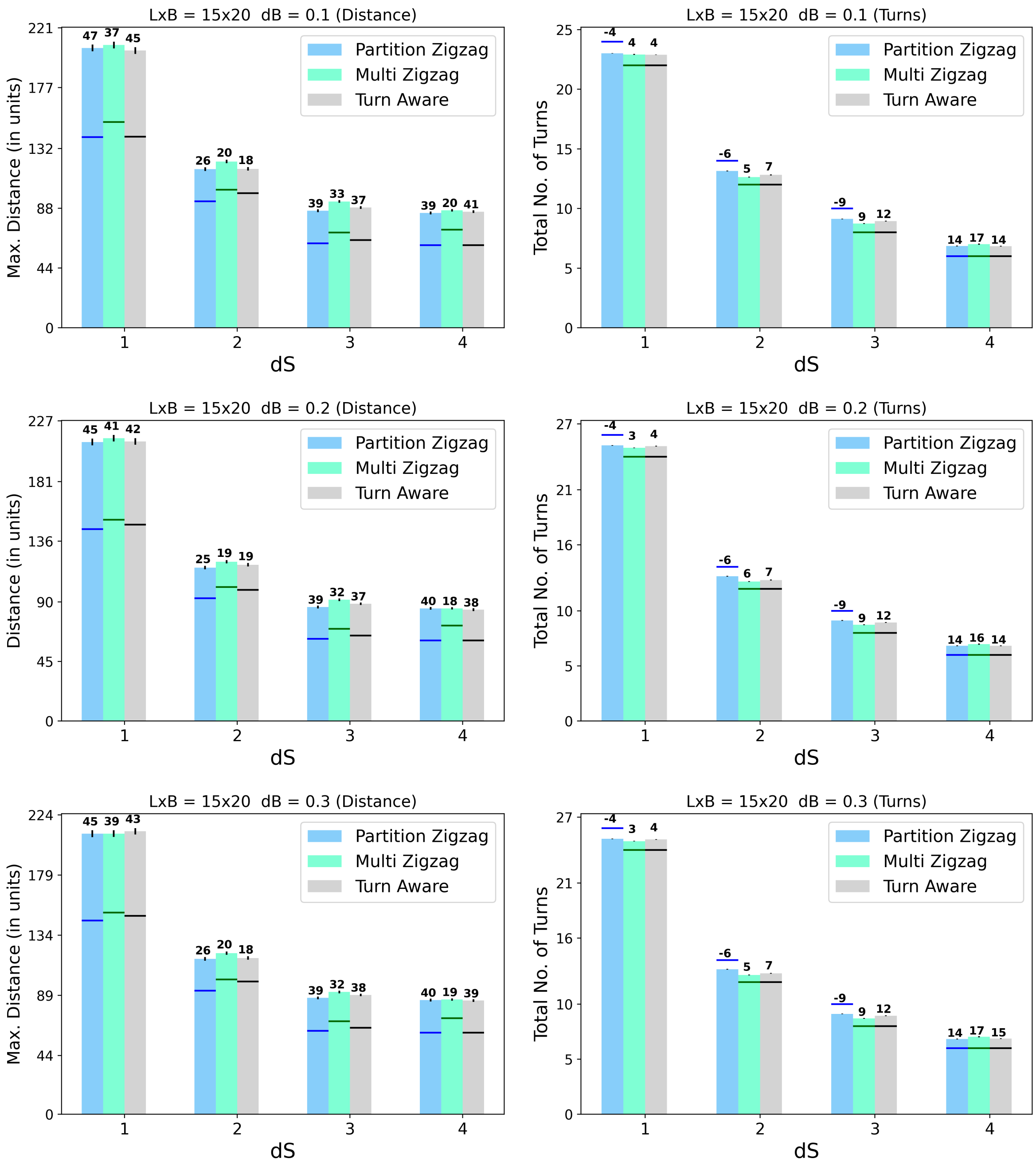

Figure 6.3: Bar plots showing the **mean** performance (with error bars) of different strategies for varying values of dS and dB with the input AOI being a rectangle of 15×20 units using **four** AUVs with blind-zone. The metrics shown for each input configuration are: the (average) maximum distance travelled by any of the 4 vehicles and the (average) total number of turns. The horizontal lines on the bar denote the performance of the same strategy if there was no failures and the values at the top of a bar denote the **percentage change** (increase or decrease) in the performance with respect to the no-failure case.

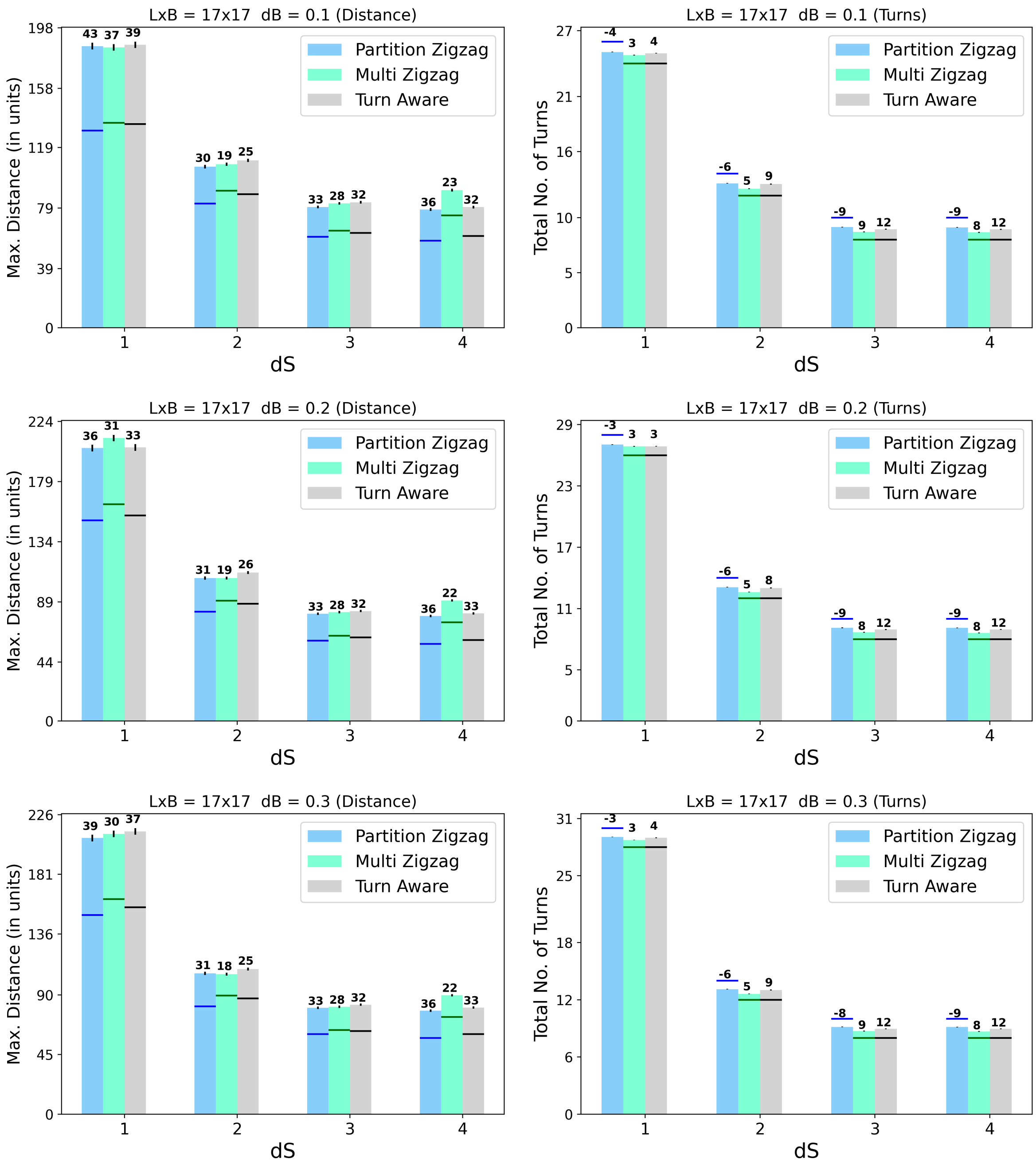

Figure 6.4: Bar plots showing the **mean** performance (with error bars) of different strategies for varying values of dS and dB with the input AOI being a square of 17×17 units using **four** AUVs with blind-zone. The metrics shown for each input configuration are: the (average) maximum distance travelled by any of the 4 vehicles and the (average) total number of turns. The horizontal lines on the bar denote the performance of the same strategy if there was no failures and the values at the top of a bar denote the **percentage change** (increase or decrease) in the performance with respect to the no-failure case.

corresponding version in the standard two AUV model from which it was extended to handle failures. We can see how worse the performance gets with failures compared to no failures. Thus, for each bar, we have plotted a horizontal line denoting the performance of the same strategy if there was no failures and also a value is shown at the top of each bar denoting the **percentage change** in the performance of the robust strategy (with respect to the no-failure case).

6.4 Discussion

We note that the results are similar for both the rectangle and square input across the various values of dS and dB. Further, we don't see a significant difference among the strategies considered. Yet, we highlight the broad conclusions for each of the considered metrics below:

- *Maximum Distance:* We find that almost always Robust Partition Zigzag (Robust $\texttt{PZ}_2$) had the lowest mean maximum distance (of any vehicle), closely followed by Robust $\texttt{TZ}_2$ and Robust $\texttt{MZ}_2$. This is not surprising given Robust $\texttt{PZ}_2$ achieves the minimal maximum distance in the case of two AUVs with no failures. Further, we notice the difference among the strategies becomes negligible as the length of the sensor footprint dS increases for a fixed value of dB.

- *Turns:* Although Robust $\texttt{TZ}_2$ achieves the lowest number of total turns in the non-failure case, we find here that mostly Robust $\texttt{MZ}_2$ achieves the lowest number of (total) turns, closely followed by Robust $\texttt{TZ}_2$ and Robust $\texttt{PZ}_2$.

  We also notice an unusual pattern in Robust $\texttt{PZ}_2$'s total number of turns – it decreases with failures in comparison to no failures. This is surprising and unintuitive at first glance. However, recall that $\texttt{CZ}_2$ (without any failure) incurred two more turns per AUV in comparison to CZ for one vehicle (Fig. 5.3). Thus, what can happen is these extra turns may be avoided if one of the vehicle fails leading to decrease in total number of turns. An example of this is shown in Fig. 6.5. Consequently, the horizontal dashes are above most of Robust PZ's bars for turns and the value at the top is negative indicating the *percentage decrease* in two AUV with failure model.

Overall, we find that in the case of failure, all the strategies perform similarly in both the considered metrics: total number of turns and maximum distance. best strategy would depend on the use case and input configuration. Specifically, if we plan to minimize the total number of turns, MZ and TZ seem to the best with MZ being slightly better overall. If the cost of turning is not significant and minimizing maximum time spent by any vehicle is the primary objective, then PZ seems to be the best strategy.

To conclude, we have laid the foundation for failure-aware planning strategies for two AUVs with nadir gaps. Handling the risk of failure in case of an arbitrary number of AUVs is significantly more challenging as one has to consider how many vehicles can fail unexpectedly and also requires a systematic communication channel between every pair of AUVs with decentralized protocols for active

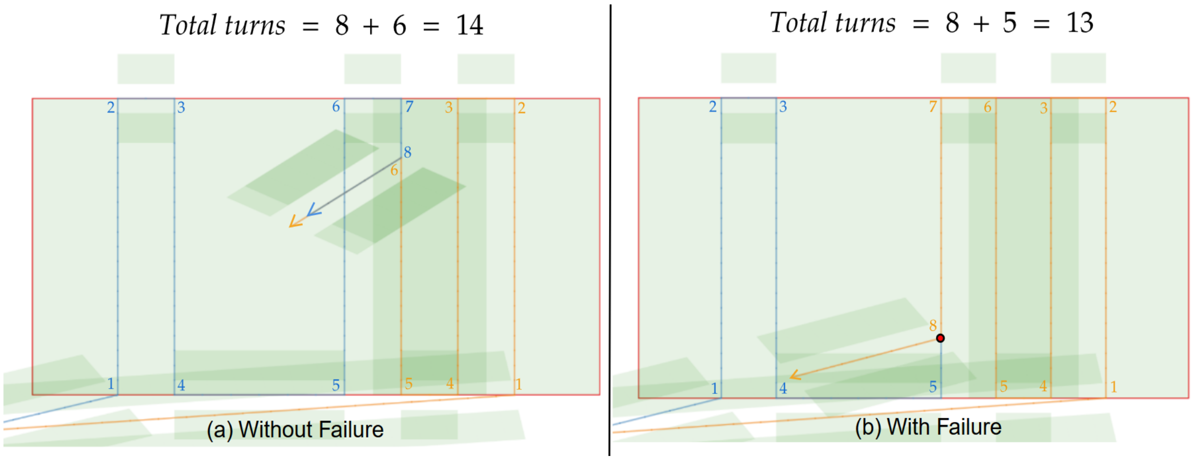

Figure 6.5: Illustration of difference in the total number of turns taken by `Complete/Partition Zigzag` strategy for two vehicles **(a) without failure** (**$\texttt{CZ}_2$**) and **(b) with failure** (**$\texttt{Robust PZ}_2$**). We notice that the number of turns can actually *decrease* with failure.

communication between vehicles alive to ensure complete coverage. The complexity of coordinating adjustments among multiple AUVs, compounded by these factors, makes failure-aware planning a complex endeavor best left for future work.

Chapter 7

Exploration with multiple AUVs

7.1 Motivation

In this chapter, we tackle the nuanced realm of coverage path planning (CPP) for *fleets* of Autonomous Underwater Vehicles (AUVs), each having their inherent nadir gaps or blind zones in sensor coverage. The leap from single to multiple AUV operations amplifies the complexity of ensuring comprehensive area coverage due to the need for intricate coordination that accounts for overlapping and uncovered areas introduced by these gaps. The quintessence of this challenge lies in devising algorithms capable of harmonizing the movements of an arbitrary number of AUVs to optimize collective coverage while acknowledging individual limitations.

The importance of this endeavor cannot be overstated, as it underpins the potential for efficient large-scale underwater exploration and surveillance. By mastering CPP with multiple AUVs, we aim to transcend the constraints of single AUV capabilities, leveraging the synergistic potential of AUV fleets to significantly reduced mission completion time.

Addressing the challenges of CPP in multi-AUV systems is not merely a technical pursuit but a critical step towards realizing the vast potential of underwater autonomous exploration. It serves as a foundation for sophisticated operations capable of addressing global challenges, from marine biodiversity conservation to the monitoring of climate change impacts on underwater ecosystems. By overcoming the hurdles presented by nadir gaps through collaborative AUV strategies, we unlock new horizons for oceanographic research and applications like mine countermeasures.

7.2 Problem Formulation

In this chapter, we are interested in the coverage of planar underwater environments using an *arbitrary* number of AUVs with nadir gaps. We define our problem of *offline* exploration in two-dimensional environment using the following tuple $\langle \mathcal{R}, N, \mathcal{S}, v, dS, dB \rangle$:

- $\mathcal{R}$ denotes the rectangular AoI of size $L \times B$ in the global frame whole of which needs to be covered once.
- N is the number of AUVs available for planning.
- $\mathcal{S}$ is the list of AUV deployment locations where $\mathcal{S}_i$ is a tuple (x_i, y_i) denoting the starting and returning coordinate for the i^{th} AUV. The size of $\mathcal{S}$ is N.
- v is the (constant) speed at which each AUV travels.
- dS is the length of sensor footprint covered by the vehicle perpendicular to its direction of motion. We model it as a scalar quantity on both sides of the motion (Fig. 3.1b).
- dB denotes the distance of blind zone left by the vehicle perpendicular to its direction of motion, modelled similarly as dS (Fig. 3.1b).

Our primary objective is to ***(a)*** *achieve* ***complete*** *coverage of the area of interest (*`AoI`*)* while our secondary objectives are either ***(b)*** *minimizing the maximum distance travelled by any of the AUVs* or ***(c)*** *minimize the total number of turns made by the AUVs*. Note that each (secondary) objective represents a distinct aspect of the mission, and *optimizing for one may compromise the other* (Yordanova et al., 2019). Thus, there may not be a single strategy optimal across all the objectives. Thus, we develop strategies tailored for each objective and empirically analyze their performance.

7.3 Strategies

We now generalize our study from two AUVs to multiple AUVs. The challenge is how to effectively use all the provided AUVs to completely explore R optimizing objectives like minimizing mission completion time or total number of turns taken by the AUVs. In this section, we provide algorithmic techniques on how to scale the strategies developed for two vehicles to multiple vehicles in a computationally efficient manner. We further call our extension of `Complete Zigzag` (`CZ`) strategy for multiple vehicles as `Partition Zigzag` (`PZ`) so that it is more descriptive.

7.3.1 Multi-Zigzag

Recall that the key idea in `Multi Zigzag` (for two AUVs) was to cover the blind-zone of a AUV using the other AUV such that both can cover each other's blind zones. This is feasible if we have even number of AUVs so that we can pair each of them so that they together follow the lawnmower strategy without leaving any gaps. The idea presented in Section 4.2.1 for two AUVs can be easily extended for multiple AUVs when we have an even number of them. Rather than discussing that, we mention below a more general strategy which is applicable to any number of AUVs (even or odd) though is suboptimal in comparison to the earlier strategy, for even number of AUVs.

Suppose we place AUVs consecutively (at multiples of dS on one side of $\mathcal{R}$ such that all of them move perpendicularly to the other side) then each AUV's right sensor footprint can cover the left blind zone of the next AUV and together they can travel leaving no gaps. We can think of this arrangement as one AUV with no blind zone having much larger sensor footprint with which we can perform a simple zigzag motion to achieve full coverage. We refer to this strategy as `MZ`. However, it is also possible that if the blind zone takes up a significant portion of the sensor footprint, then each AUV may not be able to fully cover the blind-zone of its nearby AUVs. We formalize this property below alongside the details about the strategy.

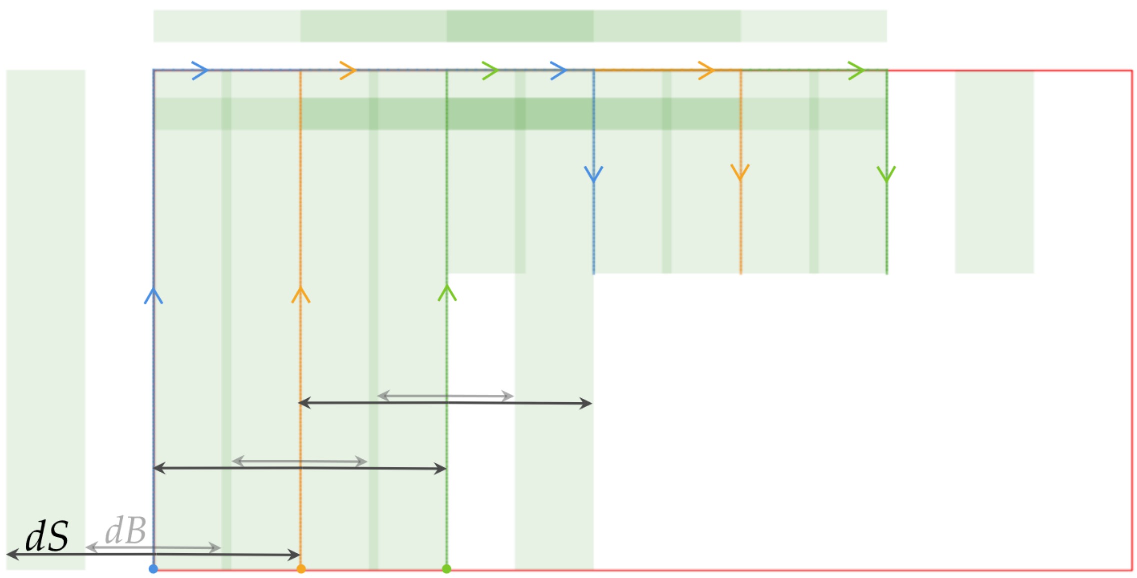

Figure 7.1: Illustration of multi-zigzag strategy in-progress using 3 blind-zone AUVs (shown in different colors) with the input rectangle denoted by red bounding box.

Theorem 3. *`MZ` strategy achieves full coverage of $\mathcal{R}$ (requiring at least 2 AUVs) if $dS \geq 2 \cdot dB$.*

Proof. Let us consider two AUVs. We place the first AUV at the bottom-left corner $(0, 0)$ and the second AUV at $(dS, 0)$ coordinate. These placements act as the initial point in $\mathcal{R}$ that they have to reach from their (respective) starting locations. The right footprint of first AUV covers the region $[dB, dS]$ while the left footprint of second AUV covers the region $[dS - dS, dS - dB] = [0, dS - dB]$ horizontally. The second AUV can cover the right blind zone of first AUV and vice versa for the first AUV if $dS - dB \geq dB \Rightarrow dS \geq 2 \cdot dB$.

As the AUVs move vertically and reach the other end, we notice that an entire rectangular strip of size $dS \times B$ is covered with an overlap of size $(dS - 2 \cdot dB) \times B$. Thus, we can consider the remaining rectangle as a new problem with reduced dimension and simulate the AUVs like initially done from the other end. We can also extend this to multiple AUVs by placing the i^{th} AUV at $\big(dS \cdot (i-1), 0\big)$ initially as AUV i's right footprint can cover the the blind zone on the left side of AUV $i+1$ and move all of them vertically to achieve entire coverage of a rectangular strip of size $dS \cdot (N-1) \times B$. $\square$

7.3.2 Partition Zigzag

While `Complete Zigzag` for two vehicles ($\mathtt{CZ}_2$) minimizes the maximum distance traveled by any vehicle, naively extending that to multiple AUVs would require N nested loops (one for each AUV) to identify the optimal waypoints for division leading to exponential time complexity. To address this, we design an efficient technique which we refer to as `PZ` and show its illustration in Fig. 7.2.

Let $P = [p_1, p_2, \ldots, p_L]$ be the path (of length L) obtained from `CZ` strategy for a *single AUV*. We would like to divide P in N parts give each part to a AUV to cover. Recall that equal division of P actually leads to unfair division of work. As we would like to finish coverage of $\mathcal{R}$ in least time possible, so the maximum work done by any AUV should be minimized.

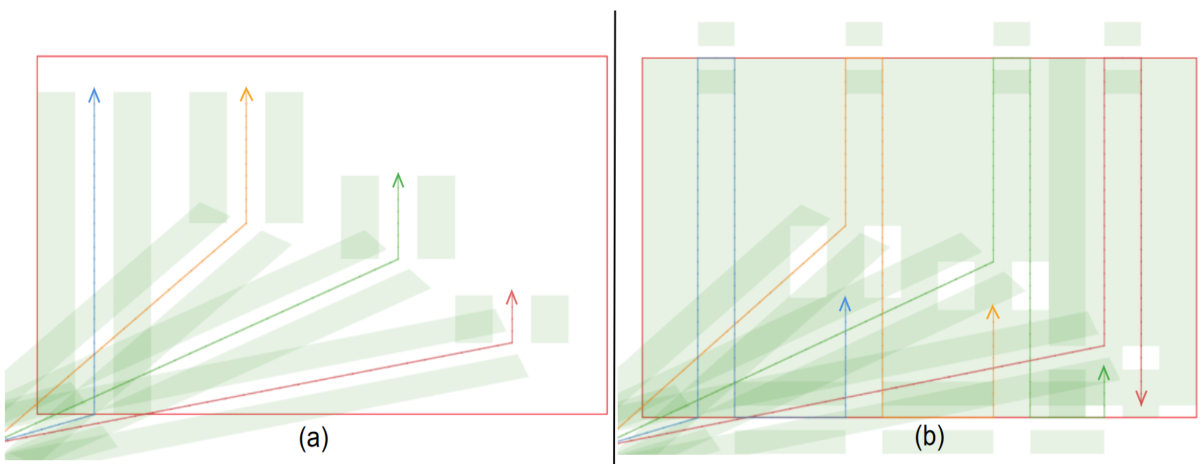

Figure 7.2: Illustration of four AUVs executing Partition Zigzag strategy: (a) Notice the starting locations of the AUVs are distributed unevenly (b) Due to uneven division of the path, the AUVs are about to complete their assigned trajectories at almost the same time.

To achieve the above objective, we had a simple approach for two AUVs where we iterated over the waypoints of P and divided the trajectory at the waypoint which was optimal with respect to our objective. However, naively extending this to multiple AUVs would required running N such nested loops leading to exponential time which would make it infeasible for practical purposes. But notice that we can create a boolean step function $f(x)$ which evaluates to *True* if it's possible to divide P into N parts such that each vehicle i travels a total distance of at most x (including starting from and returning to S_i) and returns *False* otherwise. Thus, we want to find the minimum value of x (say, x^*) such that $f(x)$ is *True*. Note that for all $x \geq x^*$, $f(x)$ will be *True* while $\forall\ x < x^*$, $f(x)$ would be *False* as by definition, x^* was the smallest value for which $f(x)$ is *True*.

If we can efficiently compute such a function for any given input x, then we can binary search to find x^*. Now we will discuss how to compute $f(x)$ efficiently. Given a value of x, we will check if it's possible to totally cover $\mathcal{R}$ by letting each AUV travel a distance of at most x. For the first AUV, we will find the highest index $j_1 \leq L$ such that the distance incurred travelling from p_1 to p_{j_1} while starting from and returning to $\mathcal{S}_1$ is $\leq x$. Let $d(p, q)$ denote the distance between two points p, q. To compute this, we can simply iterate over P starting from p_1 and at each waypoint p_k calculate the distance from $\mathcal{S}_1$ to p_1, p_1 to p_k through $p_z (1 \leq z < k)$ and the distance from p_k to $\mathcal{S}_1$. Thus after finding the highest index j_1 for the first AUV, we repeat the same process for the second AUV starting from j_1 ie., finding the highest index j_2 such that it travels $\leq x$ distance. In general, for a AUV i, we find the highest index $j_i \leq L$ such that, starting from and returning to $\mathcal{S}_i$, it covers $P[p_{j_{i-1}} : p_{j_i}]$ portion of the path[1] P while incurring a distance of $\leq x$. Thus, for AUV i, at waypoint p_k, we have to compute the following (illustrated in Fig. 7.3):

$$d(\mathcal{S}_i, p_{j_{i-1}}) + \sum_{z\,=\,j_{i-1}}^{k-1} d(p_z, p_{z+1}) + d(p_k, \mathcal{S}_i)$$

Note that the first and last term in the above summation are constant time operations while $d(P[p_{j_{i-1}} : p_k])$ (i.e., the middle term) can be computed efficiently by maintaining (and updating) a running sum[2]. In the end, if j_N is L (that is, the last AUV can reach the end of path P within the allowed distance threshold x), then we return *True* (and *False* otherwise). Hence, we can evaluate $f(x)$ for any x in $O(L)$ (i.e., linear time) by just traversing over the waypoints of P.

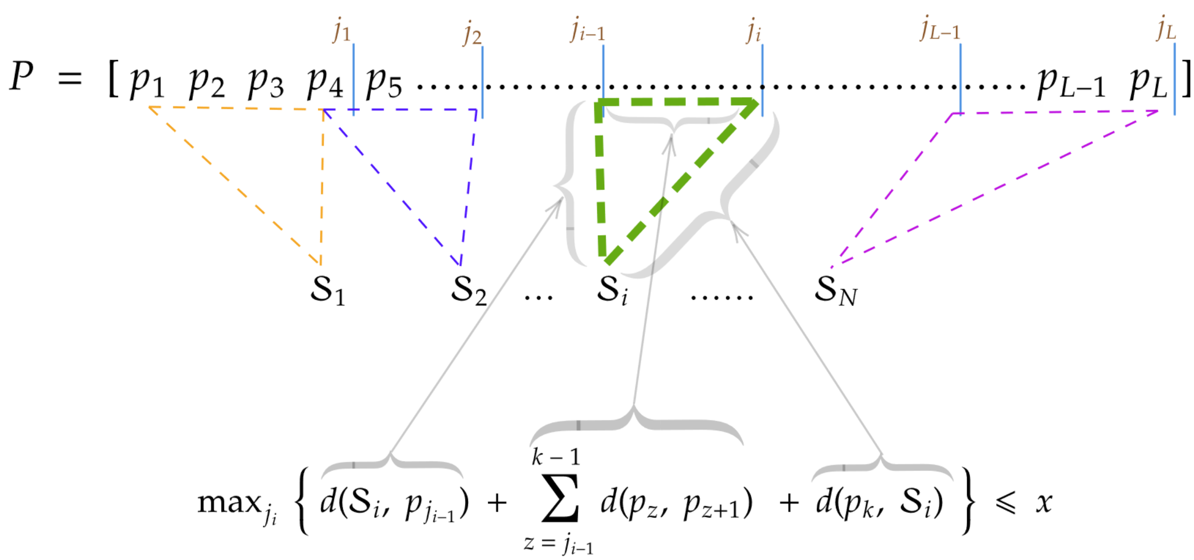

Figure 7.3: Illustration of how P is divided into N segments in the Partition Zigzag strategy for multiple AUVs, given a maximum distance threshold x for each AUV to travel.

[1] Assume $j_0 = 1$.
[2] or prefix sum.

To obtain x^*, we need to evaluate f in a suitable range $x \in [x_{low}, x_{high}]$. While one can come up with reasonable range estimates for x_{low}, x_{high} based on the input parameter values, another simple way to set these parameters is to set x_{low} to be a negligibly small number, say $\epsilon = 10^{-4}$, and x_{high} to a very large number, say 10^9. These limits, while conservative, ensure that the final solution will always lie within the range. Given that binary search only takes logarithmic time, even with such extreme values of x_{low} and x_{high}, it will converge to x^* in a moderate number of iterations (≤ 100 iterations). After finding the optimal value x^*, we again run $f(x^*)$ to compute the indices j_i for all AUVs and assign their respective paths to them. The path of AUV i would be

$$P_i = [\mathcal{S}_i, p_{j_{i-1}}, p_{j_{i-1}+1}, p_{j_{i-1}+2}, \ldots, \mathcal{S}_i]$$

This way, we achieve the original objective we aimed for (same as in the case of *two* AUVs): attaining complete coverage of $\mathcal{R}$ while minimizing the maximum distance travelled by any AUV (consequently, minimizing the overall completion time). An example execution of Partition Zigzag is shown in Fig. 7.2

7.3.3 Turn-Aware Zigzag

Similar to `Complete Zigzag` for two AUVs, we could efficiently computer `Turn-Aware Zigzag` strategy in the case of two AUVs by iterating over all the waypoints in P and checking which maintains the least number of turns. However, as with `Partition Zigzag`, naively extending this to multiple AUVs would be impractical. However, we can take inspiration from the way `Partition Zigzag` has been formulated for multiple AUVs in the previous subsection.

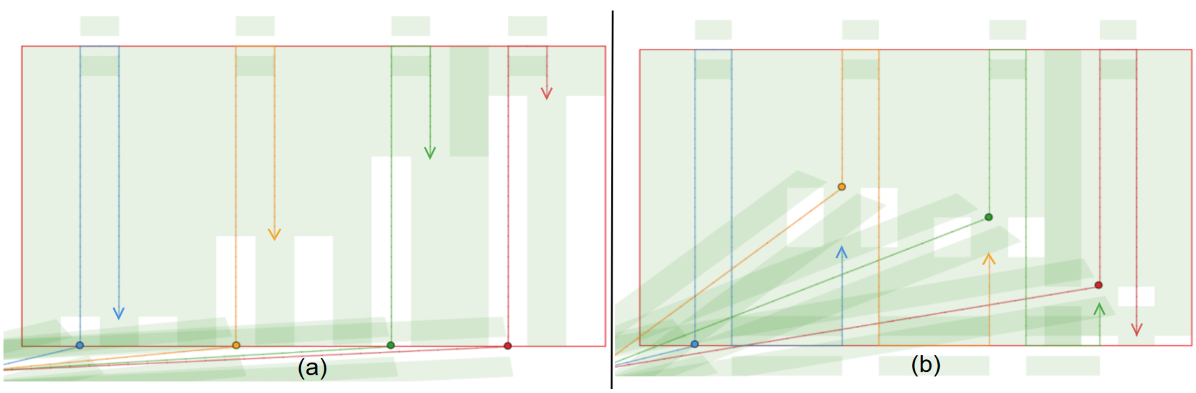

Figure 7.4: Comparison of `TZ` strategy (a) with `PZ` strategy (b) on the same input. The arrows denote the direction of the path followed by each AUV while the small colored circle (with black border) denotes the starting location of each AUV. (a) Illustration of four AUVs executing Turn-Aware Zigzag strategy. Note that starting (and ending) location of each AUV is a waypoint where a turn occurs. (b) Illustration of the same four AUVs executing Partition Zigzag strategy, similar to Fig. 5.3(b). Note the difference in the starting locations of the AUVs compared to when they are following Turn-Aware strategy.

We can define a function $f(x)$ exactly as earlier. But to explicitly take care of turns, for each AUV i, we need to find the highest index j_i such that p_{j_i} **is a turning point** in P and distance incurred till there (including beginning from and returning to $\mathcal{S}_i$) is $\leq x$. It is important for any AUV to end its trajectory at a waypoint which was a turning point in P so that no additional turns are incurred (justification for this has been provided earlier in section 4.2.3). The next AUV's initial point would be p_{j_i+1} (and not p_{j_i} as in Parition Zigzag) because $p_{j_i} \to p_{j_i+1}$ is a turn which was not a useful maneuver but was only needed originally to reach the next important waypoint. Thus, the next AUV $(i+1)$ can directly reach p_{j_i+1} from $\mathcal{S}_{i+1}$ to begin exploring its assigned path which will not hamper the complete coverage of $\mathcal{R}$. Finally, like earlier, we can binary search on $f(x)$ to find the maximal distance x^* that any AUV would have to travel without increasing the total number of turns (i.e., the number of turns required by a single AUV to follow `CZ` strategy). We refer to this strategy as `TZ` and show its illustration in Fig. 7.4.

Corollary. *`TZ` for arbitrary number of AUVs incurs the same number of total turns as `CZ` for one AUV.*

We note that the *resulting trajectory* followed by the vehicles (inside $\mathcal{R}$) in both `PZ` and `TZ` is equivalent to the trajectory followed by a single AUV in `CZ`; thus, the two strategies inherit the same coverage guarantees as `Complete Zigzag`:

Corollary. *Both `PZ` and `TZ` achieve full coverage of $\mathcal{R}$ when $dS \geq 3 \cdot dB$.*

7.4 Simulation Results for Multiple AUVs

To evaluate the performance of the strategies developed for multiple AUVs, we perform simulations on different input parameters following exactly the same setup as described earlier in Section 3.4, unless mentioned otherwise below. We consider varying number of AUVs for each input configuration: 4 and 8. While the input area (of size $L \times B$) was represented from coordinates $(0, 0)$ to (L, B), the starting and returning location for AUV i was $(-i, -5)$.

Given that all the strategies being evaluated (`MZ, TZ, PZ`) achieve full coverage under their required assumptions, we skip plotting their coverage percentage and showcase their performance on total number of turns performance and maximum distance travelled by any vehicle in Fig. 7.5, 7.6, 7.7, 7.8.

To further understand the impact of the number of vehicles, we consider a huge area of size 100×100 unit sq. and evaluate the performance of the strategies for $8, 16, 32$ AUVs each, shown in Fig. 7.9. In all our simulations, consistent with our previous findings (for two AUVs), we find that `PZ` achieves the lowest maximum distance by any AUV throughout followed by `TZ` while `MZ` performs much poorly in this aspect in comparison. Similarly, for number of total turns, we find `TZ` performs the best throughout while there is no dominant strategy between `MZ` and `PZ` as one is better sometimes and worse other times (dependant on the input parameters).

Collision Avoidance: As the AUVs under consideration do not have the capability to sense other vehicles or objects in their vicinity, so we ensure collision avoidance by sufficiently spacing apart their *starting locations* (as stated above) and from the fact that there is no intersection between the trajectories (generated by our strategies) they have to follow in the `AoI`. In this way, the given area is partitioned into N (disjoint) parts for strategies PZ and $\mathtt{TZ}_k$ where each part is uniquely assigned to one of the vehicles (chronologically). Thus, each of vehicles safely follows their assigned paths and no explicit coordination between them is required.

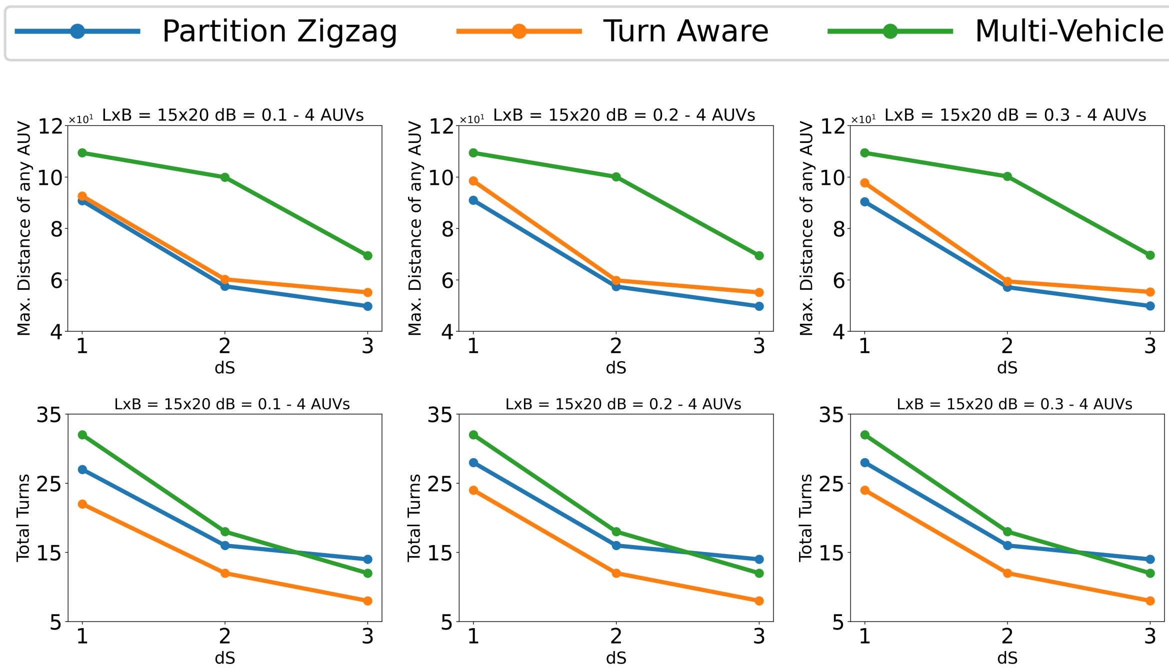

Figure 7.5: Line plots denoting the maximum distance travelled by any of the 4 vehicles and total number of turns performed by different strategies for varying values of dS and dB with the input AoI being a rectangle of 15×20 units using **four** AUVs with blind-zone.

7.4.1 Discussion

The relative performance of the different strategies was found to be consistent across the environments (rectangle of dimension 15×20 units and square of dimension 17×17 units) and the different values of dS, dB considered. These findings remain consistent even if we vary the number of vehicles from 4 to 8 to even 16 and 32[3]. For each metric, we see a clear distinction in the performance of the strategies. We discuss the performance of strategies on each of the considered metrics below:

- *Maximum Distance:* We find that Partition Zigzag (PZ) achieve the lowest maximum distance, closely followed by TZ but MZ has significantly higher maximum distance. The superior performance of PZ is expected as it is designed to minimize the maximum distance travelled by any vehicles by incorporating distance from their starting (returning) locations into their coverage trajectories.

[3]32 AUVs was only used for the largest input of 100×100 units.

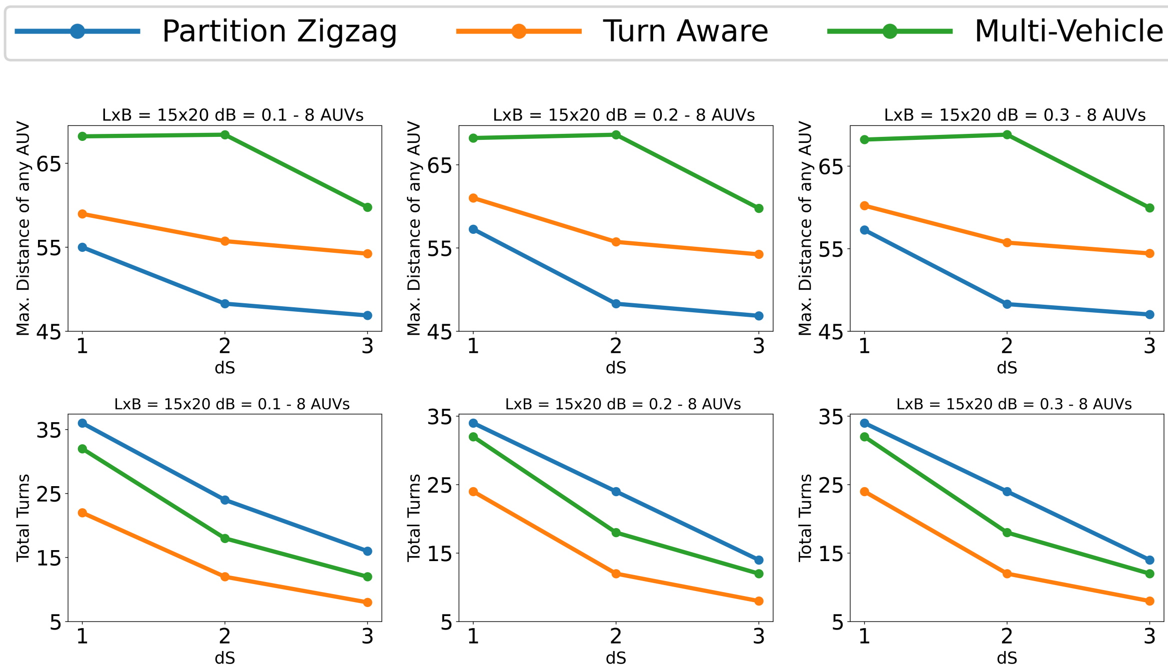

Figure 7.6: Line plots denoting the maximum distance travelled by any of the 8 vehicles and total number of turns performed by different strategies for varying values of dS and dB with the input `AoI` being a rectangle of 15×20 units using **four** AUVs with blind-zone.

- *Turns:* We find that `TZ` achieves the lowest number of (total) turns while $\mathtt{MZ}_k$ and `PZ` show mixed performance depending on input parameters. Regarding `PZ` resulting in more turns than `TZ`, we had noticed earlier that it might incur two more turns per (each) AUV as shown earlier (in Fig. 5.3).

Overall, we find that the best strategy would depend on the use case. If we plan to minimize the total number of turns, `TZ` is the most promising strategy as we had developed it accordingly. When minimizing the maximum time spent by any vehicle (equivalently, the mission completion time) is the primary objective, then `PZ` would be the best strategy. These findings are consistent across scaling of the size of the `AoI` and number of vehicles.

7.4.2 Maximal Number of AUVs

A natural question to ask when we have the availability of multiple AUVs is whether all of them can be fruitfully used for complete coverage of $\mathcal{R}$? Here, by fruitful usage we mean all of them have a positive contribution to the coverage of $\mathcal{R}$. Is it the case that we can keep increasing the number of AUVs to decrease mission completion time? Note that all the AUVs have a fixed starting position which would be the launching hub so they cannot directly start from arbitrary locations.

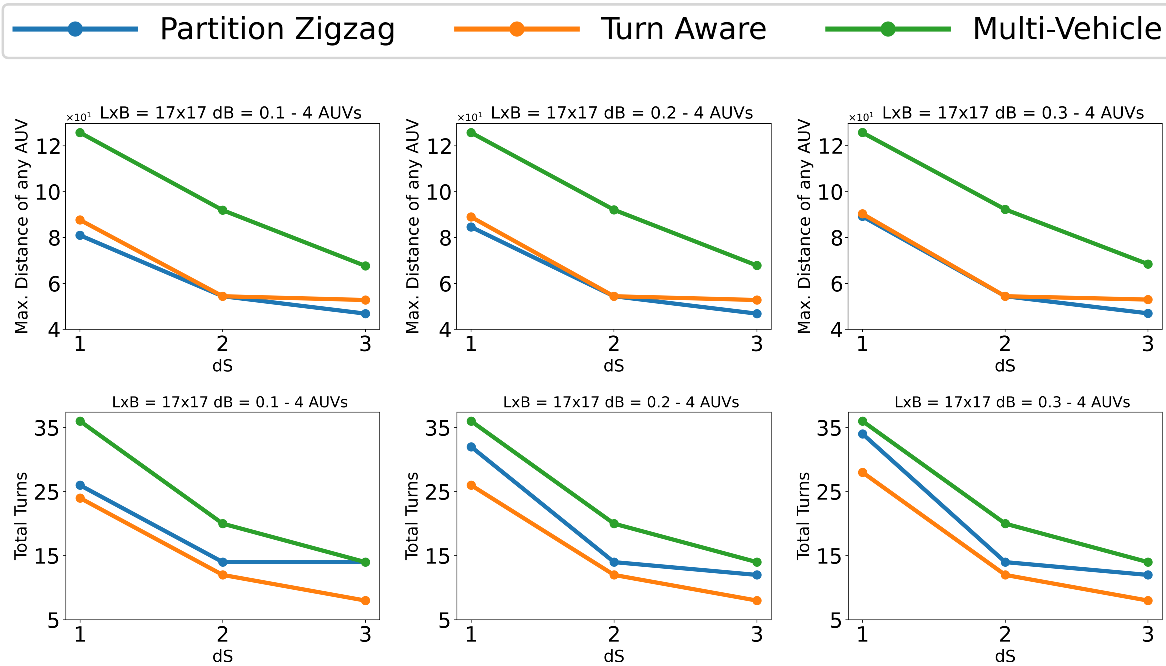

Figure 7.7: Line plots denoting the maximum distance travelled by any of the 4 vehicles and total number of turns performed by different strategies for varying values of dS and dB with the input `AoI` being a *square* of 17×17 units using **four** AUVs with blind-zone.

Due to the fixed starting locations and the need for the AUVs to return, the answer to the above question is negative. Any strategy's performance after a certain number of AUVs stagnates i.e., the performance of the strategy stops improving and remains at a constant level. Thus, adding more AUVs beyond this threshold does not result in any increase in performance. This phenomenon is more commonly referred to as the "performance plateau."

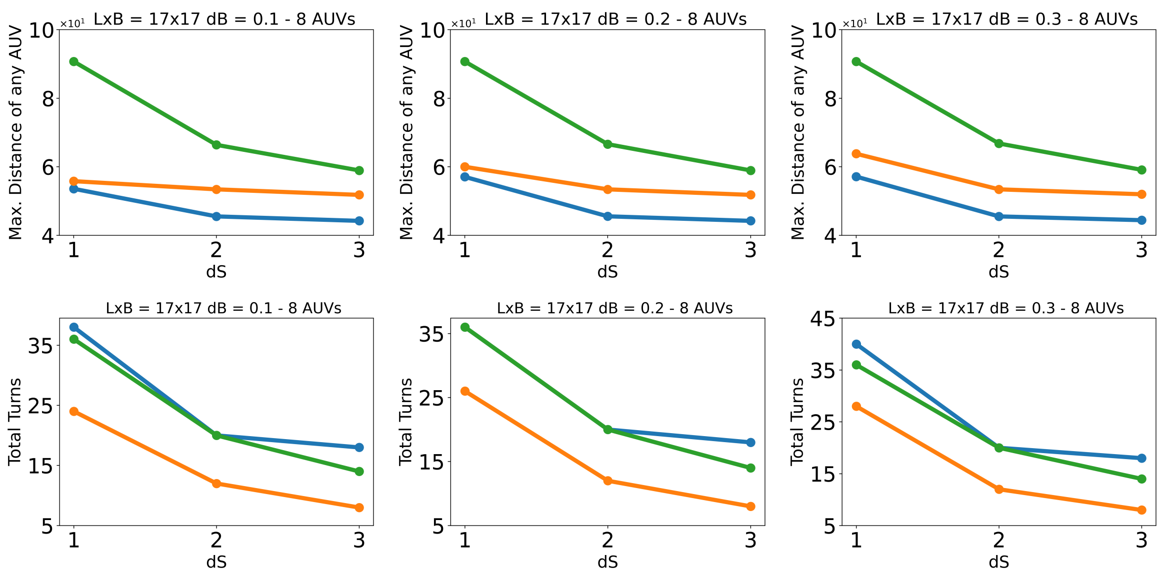

Figure 7.8: Line plots denoting the maximum distance travelled by any of the 8 vehicles and total number of turns performed by different strategies for varying values of dS and dB with the input `AoI` being a *square* of 17×17 units using **eight** AUVs with blind-zone

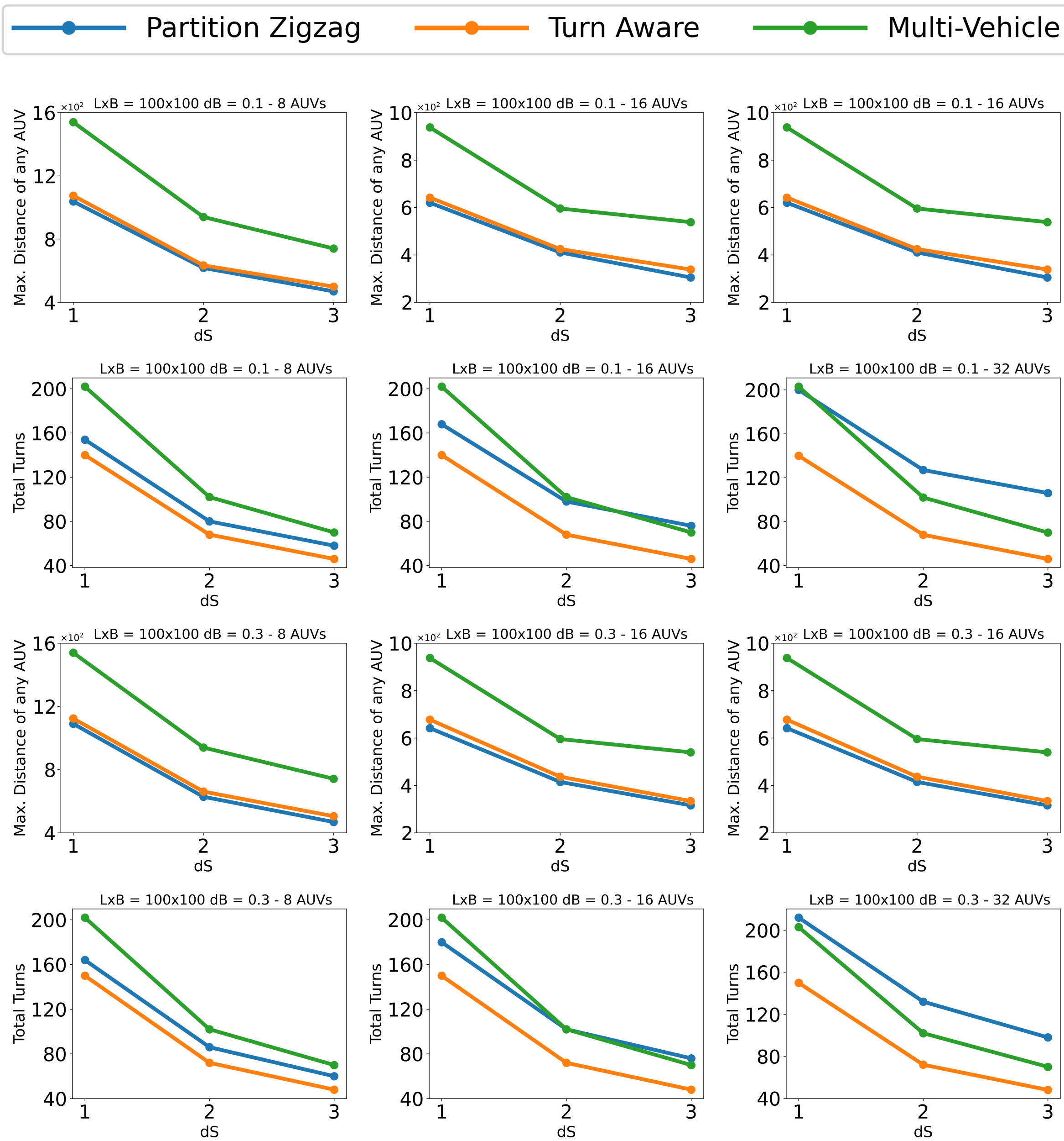

Figure 7.9: Line plots denoting the maximum distance travelled by any of the vehicles and total number of turns performed by the different strategies for varying values of dS and dB with a gigantic input `AoI` being 100×100 units. The number of AUVs used vary with column, with first column showing plots with 8 AUVs, second with 16 and third with 32 AUVs.

A natural question to ask next is given an input configuration, can we find the maximal number of AUVs required to arrive at the minimal overall completion time? That is, for a given strategy, irrespective of the number of AUVs, how much time at the least will be required for complete coverage of $\mathcal{R}$. Fortunately, we can answer this without incurring a significant overhead. We can simply binary search over the number of AUVs as any strategy's completion time is non-decreasing with increase in number of AUVs. Thus, we can efficiently compute this using `PZ` as the underlying strategy since it minimizes the maximum distance travelled by any AUV.

Using exactly the same input configurations as earlier, we show the change in performance of different strategies (`PZ, TZ, MZ`) as the number of AUVs varies in Fig. 7.10 and 7.11. The number of AUVs considered in the x-axis is till where the maximal distance travelled by any AUV decreases (for `PZ`) with the last two data points showing the same distance implying the maximal number of AUVs threshold has been crossed.

In terms of the maximum distance travelled by any AUV, we find significant difference in performance between `PZ` and `MZ` initially. Whereas, `TZ` comes close to `PZ` but it converges much earlier with its least maximum distance (by any AUV) always being 15% higher than that of `PZ`. While `MZ`'s maximum distance decreases significantly with increase in the number of AUVs, it is always more than that of `TZ` and much worse (up to 50%) than `PZ`. Through `PZ`, we found the maximal number of AUVs that can be used effectively for our problem setting (i.e., more than that would not offer any further reduction in mission completion time). Regarding turns, `TZ` *consistently incurs the same number regardless of AUV count*. Conversely, `PZ`'s turns increase with more AUVs, while `MZ`'s number of turns remains constant but much more than `TZ`.

Overall, this adds more support to the strengths of our two best strategies: `TZ` for minimal total number of turns and `PZ` for minimizing mission completion time (though at the cost of more turns).

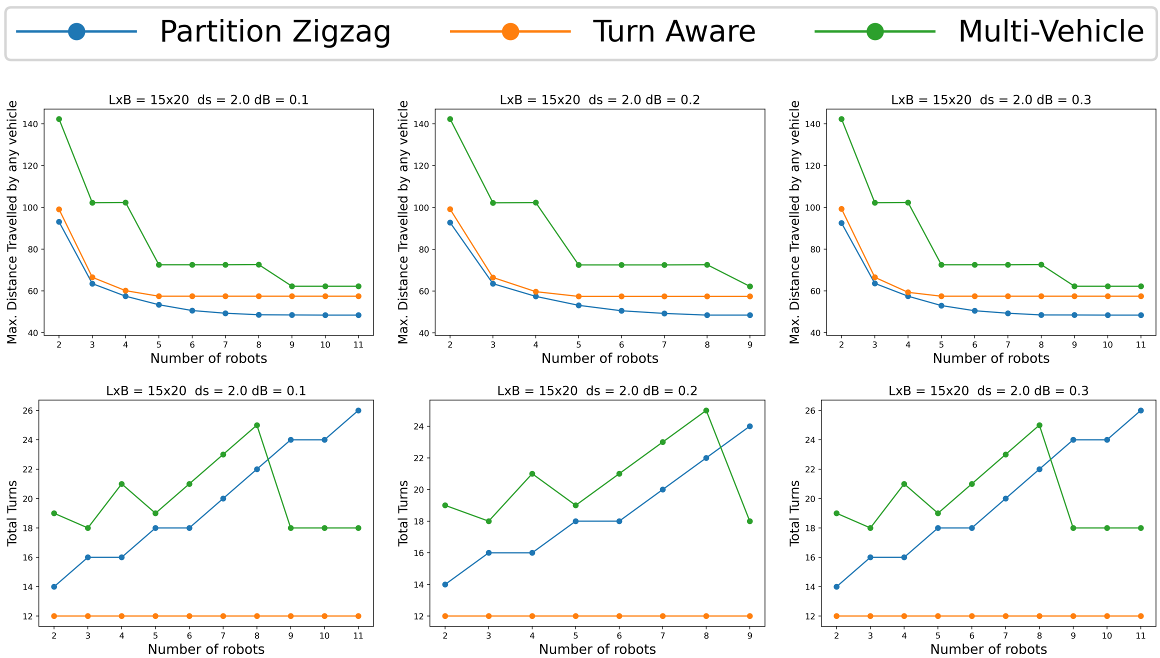

Figure 7.10: Line plots denoting how the maximum distance and total number of turns vary as the number of AUVs increase for fixed value of dS and dB with the input AOI being a rectangle of dimensions 15×20.

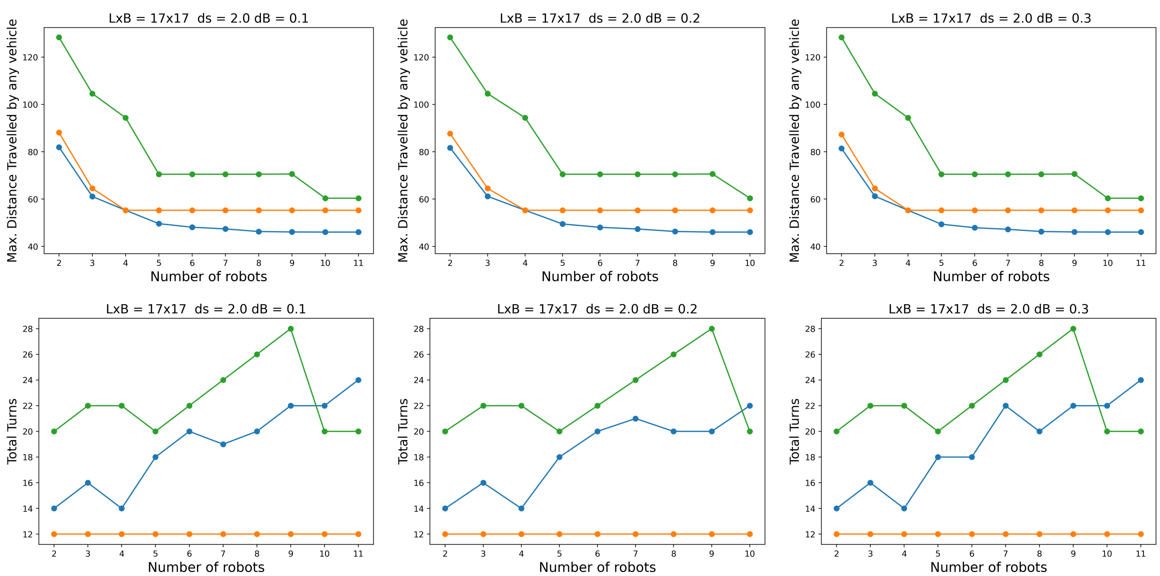

Figure 7.11: Line plots denoting how the maximum distance and total number of turns vary as the number of AUVs increase for fixed values of dS and dB with the input AOI being a square of size 17×17 units.

Chapter 8

Conclusion and Future Work

In this thesis, we studied the fundamental version of coverage path planning (CPP) with the practical constraint of *nadir gaps*. Our focus was on achieving complete coverage while secondary objectives were either to minimize the mission completion time or the number of turns performed by the AUVs. We first studied planning strategies for single AUV, We proposed some new strategies for CPP with single AUV and also discussed the existing strategies for it. We found that the strategy which we named `Complete Zigzag` and is used in practice performed the best across all the environments and metrics in our simulations. We also theoretically analyzed its overlap concluding with the conjecture that it should occur the same overlap as an optimal single-AUV strategy.

Going beyond single-AUV, we took the first steps and studied CPP with two AUVs. We discussed how to extend `Complete Zigzag` to two AUVs while either optimizing for minimizing the maximum distance travelled by any AUV or the total number of turns performed by the AUVs. We developed strategies tailored to each metric while ensuring that they offer *complete coverage*.

Apart from simple offline planning, we also covered *robust planning* – where failure of some members of the AUV team can be compensated by others – with two AUVs. We found that the performance of the fault-tolerant version of `Turn-Aware Zigzag` and `Complete Zigzag` was comparable to their original counterparts, both in terms of the distance travelled and the turns incurred. With (randomized) failures, the performance all the strategies considered turned out to be similar on average.

Finally, we provide algorithmic techniques to scale the strategies developed for two AUVs to an arbitrary number of AUVs which is the main contribution of this thesis. We found that the performance of the strategies varies depending upon the metric used for evaluation and the practitioner's use case. For minimizing overall completion time, we found Partition Zigzag (`PZ`) performs the best with significant margin over others while Turn-Aware Zigzag (`TZ`) was the best strategy for minimizing the total number of turns. We not only grounded them theoretically but also validated their key properties through extensive simulations. In summary, our work offers insights and novel strategies for large-scale underwater exploration with a focus on *complete coverage*. While this thesis took the first steps towards addressing the challenges arising from the deployment of multiple AUVs in the context of CPP, we focused on the fundamental setting with static rectangular seabed without obstacles and reliable However, as AUVs are deployed in the real-world, additional practical constraints can be considered for future work:

- While we consider a rectangular seabed, researchers can also explore coverage of complex, non-rectangular planar areas using decomposition techniques like voronoi partitioning (Fang and Anstee, 2010).
- We consider the sonar detector to be perfect. However, this might not always be the case and the sensor may not always produce binary signal. In practice, we might actually have an imperfect detector defining a probability distribution over the sensor range for mine detection (Abreu et al., 2017; Morin et al., 2013; Zhou et al., 2020; Cai et al., 2022). Thus, exploring CPP with an imperfect and probablistic sensor is in important direction of future work.
- We considered a static seabed but sand ripples might occur in the water which can impact orientation and movement of the AUVs and derail them from their planned paths (Yordanova et al., 2019). Thus, incorporating the effect of sand ripples is another key direction for reliable data collection for full coverage.
- While we explored the foundations for failure-aware planning strategies using two AUVs with nadir gaps, handling the risk of failure in case of an arbitrary number of AUVs is significantly more challenging as one has to consider how many vehicles can fail unexpectedly and also requires a systematic communication channel. These factors makes failure-aware planning a complex endeavor best left for future work.
- In other applications, obstacles may be present or the environment may also not be two-dimensional. Exploring coverage path planning in the presence of obstacles or three dimensional environment with a suitable sensor model can also be considered based on the (downstream) use case.

We hope our work inspires a plethora of research in coverage path planning.

Publications

Related

1. **Nikhil Chandak**, Charu Sharma, and Kamalakar Karlapalem. Coverage Path Planning using Multiple AUVs with Nadir Gap. AAMAS Autonomous Robots and Multirobot Systems (ARMS) Workshop 2024.

Others

1. **Nikhil Chandak**, Shashwat Goel, and Dominik Peters. Proportional Aggregation of Preferences for Sequential Decision Making. (**Oral**) AAAI Conference on Artificial Intelligence 2024. **Outstanding Paper Award**.

2. **Nikhil Chandak**, Kenny Chour, Sivakumar Rathinam, and R. Ravi. Informed Steiner Trees: Sampling and Pruning for Multi-Goal Path Finding in High Dimensions. IEEE Transactions on Automation Science and Engineering 2023 and in proceedings of IEEE International Conference on Robotics and Automation 2024.

Bibliography

Nuno Abreu, Nuno Cruz, and Aníbal Matos. 2017. Accounting for uncertainty in search operations using auvs. In *2017 IEEE Underwater Technology (UT)*, pages 1–8. IEEE.

Antonio Adaldo, Sina Sharif Mansouri, Christoforos Kanellakis, Dimos V Dimarogonas, Karl H Johansson, and George Nikolakopoulos. 2017. Cooperative coverage for surveillance of 3d structures. In *2017 IEEE/RSJ International Conference on Intelligent Robots and Systems (IROS)*, pages 1838–1845. IEEE.

Gustavo SC Avellar, Guilherme AS Pereira, Luciano CA Pimenta, and Paulo Iscold. 2015. Multi-uav routing for area coverage and remote sensing with minimum time. *Sensors*, 15(11):27783–27803.

Fotios Balampanis, Ivan Maza, and Anibal Ollero. 2017. Area partition for coastal regions with multiple uas. *Journal of Intelligent & Robotic Systems*, 88(2):751–766.

Francesco Baralli, Michel Couillard, Jesus Ortiz, and Darwin G Caldwell. 2013. Gpu-based real-time synthetic aperture sonar processing on-board autonomous underwater vehicles. In *2013 MTS/IEEE OCEANS-Bergen*, pages 1–8. IEEE.

Chang Cai, Jianfeng Chen, Qingli Yan, Fen Liu, and Rongyan Zhou. 2022. A prior information-based coverage path planner for underwater search and rescue using autonomous underwater vehicle (auv) with side-scan sonar. *IET Radar, Sonar & Navigation*, 16(7):1225–1239.

Zuo Llang Cao, Yuyu Huang, and Ernest L Hall. 1988. Region filling operations with random obstacle avoidance for mobile robots. *Journal of Robotic systems*, 5(2):87–102.

David W Casbeer, Derek B Kingston, Randal W Beard, and Timothy W McLain. 2006. Cooperative forest fire surveillance using a team of small unmanned air vehicles. *International Journal of Systems Science*, 37(6):351–360.

Howie Choset. 2001. Coverage for robotics–a survey of recent results. *Annals of mathematics and artificial intelligence*, 31(1):113–126.

Howie Choset and Philippe Pignon. 1998. Coverage path planning: The boustrophedon cellular decomposition. In *Field and service robotics*, pages 203–209. Springer.

Matthew Coombes, Wen-Hua Chen, and Cunjia Liu. 2017. Boustrophedon coverage path planning for uav aerial surveys in wind. In *2017 International conference on unmanned aircraft systems (ICUAS)*, pages 1563–1571. IEEE.

Wesley DeBusk. 2010. Unmanned aerial vehicle systems for disaster relief: Tornado alley. In *AIAA Infotech@ Aerospace 2010*, page 3506.

Cheng Fang and Stuart Anstee. 2010. Coverage path planning for harbour seabed surveys using an autonomous underwater vehicle. In *OCEANS'10 IEEE SYDNEY*, pages 1–8. IEEE.

Per Espen Hagen. 2011. Gap filler sensors for sas. In *OCEANS'11 MTS/IEEE KONA*, pages 1–6. IEEE.

Per Espen Hagen and Roy Edgar Hansen. 2007. Area coverage rate of synthetic aperture sonars. In *OCEANS 2007-Europe*, pages 1–5. IEEE.

Roy Edgar Hansen, Hayden John Callow, Torstein Olsmo Sabo, and Stig Asle Vaksvik Synnes. 2011. Challenges in seafloor imaging and mapping with synthetic aperture sonar. *IEEE Transactions on geoscience and Remote Sensing*, 49(10):3677–3687.

Mahdi Hassan and Dikai Liu. 2017. Simultaneous area partitioning and allocation for complete coverage by multiple autonomous industrial robots. *Autonomous Robots*, 41(8):1609–1628.

Muzaffer Kapanoglu, Mete Alikalfa, Metin Ozkan, Osman Parlaktuna, et al. 2012. A pattern-based genetic algorithm for multi-robot coverage path planning minimizing completion time. *Journal of intelligent manufacturing*, 23(4):1035–1045.

Chan Sze Kong, New Ai Peng, and Ioannis Rekleitis. 2006. Distributed coverage with multi-robot system. In *Proceedings 2006 IEEE International Conference on Robotics and Automation, 2006. ICRA 2006.*, pages 2423–2429. IEEE.

Vladimir J Lumelsky, Snehasis Mukhopadhyay, and Kang Sun. 1990. Dynamic path planning in sensor-based terrain acquisition. *IEEE Transactions on Robotics and Automation*, 6(4):462–472.

Sandeep Manjanna, Alberto Quattrini Li, Ryan N Smith, Ioannis Rekleitis, and Gregory Dudek. 2018. Heterogeneous multi-robot system for exploration and strategic water sampling. In *2018 IEEE International Conference on Robotics and Automation (ICRA)*, pages 4873–4880. IEEE.

Luis Merino, Fernando Caballero, J Ramiro Martínez-de Dios, Iván Maza, and Aníbal Ollero. 2012. An unmanned aircraft system for automatic forest fire monitoring and measurement. *Journal of Intelligent & Robotic Systems*, 65(1):533–548.

Michael Morin, Irène Abi-Zeid, Yvan Petillot, and Claude-Guy Quimper. 2013. A hybrid algorithm for coverage path planning with imperfect sensors. In *2013 IEEE/RSJ International Conference on Intelligent Robots and Systems*, pages 5988–5993. IEEE.

Janosch Nikolic, Michael Burri, Joern Rehder, Stefan Leutenegger, Christoph Huerzeler, and Roland Siegwart. 2013. A uav system for inspection of industrial facilities. In *2013 IEEE Aerospace Conference*, pages 1–8. IEEE.

José Manuel Palacios-Gasós, Zeynab Talebpour, Eduardo Montijano, Carlos Sagüés, and Alcherio Martinoli. 2017. Optimal path planning and coverage control for multi-robot persistent coverage in environments with obstacles. In *2017 IEEE International Conference on Robotics and Automation (ICRA)*, pages 1321–1327. IEEE.

Sonia Waharte and Niki Trigoni. 2010. Supporting search and rescue operations with uavs. In *2010 International Conference on Emerging Security Technologies*, pages 142–147. IEEE.

David P Williams. 2010. On optimal auv track-spacing for underwater mine detection. In *2010 IEEE International Conference on Robotics and Automation*, pages 4755–4762. IEEE.

Anqi Xu, Chatavut Viriyasuthee, and Ioannis Rekleitis. 2014. Efficient complete coverage of a known arbitrary environment with applications to aerial operations. *Autonomous Robots*, 36(4):365–381.

Fumio Yasutomi, Makoto Yamada, and Kazuyoshi Tsukamoto. 1988. Cleaning robot control. In *Proceedings. 1988 IEEE International Conference on Robotics and Automation*, pages 1839–1841. IEEE.

Veronika Yordanova and Bart Gips. 2020. Coverage path planning with track spacing adaptation for autonomous underwater vehicles. *IEEE Robotics and Automation Letters*, 5(3):4774–4780.

Veronika Yordanova, Bart Gips, Thomas Furfaro, and Samantha Dugelay. 2019. Coverage path planning for mine countermeasures: Adapting track orientation. In *OCEANS 2019-Marseille*, pages 1–7. IEEE.

Mingxi Zhou, Jianguang Shi, and Lin Zhao. 2020. Towards the development of an online coverage path planner for uuv-based seafloor survey using an interferometric sonar. In *2020 IEEE/OES Autonomous Underwater Vehicles Symposium (AUV)*, pages 1–5. IEEE.